IOWA STATE UNIVERSITY
Digital Repository

2004

Protein-protein interaction and electron transfer: case of cytochrome f and cytochrome c6

Tijana Žarković Grove
Iowa State University

Follow this and additional works at: https://lib.dr.iastate.edu/rtd

Part of the <u>Biochemistry Commons</u>, and the <u>Physical Chemistry Commons</u>

NOTE TO USERS

Protein-protein interaction and electron transfer:
Case of cytochrome f and cytochrome c_6

by

Tijana Žarković Grove

A dissertation submitted to the graduate faculty

in partial fulfillment of the requirements for the degree of

DOCTOR OF PHILOSOPHY

Major: Physical Chemistry

Program of Study Committee:
Gordon J. Miller, Major Professor
Amy H. Andreotti
James H. Espenson
Mark S. Gordon
Xueyu Song

Iowa State University

Ames, Iowa

2004

All scholarly activities described in this thesis were carried under the direct supervision and
support of Prof. Nenad M. Kostić, Department of Chemistry.

Graduate College
Iowa State University

This is to certify that the doctoral dissertation of

Tijana Žarković Grove

has met the dissertation requirements of Iowa State University

Signature was redacted for privacy.

Major Professor

Signature was redacted for privacy.

For the Major Program

But blessed is the man who
trusts in the Lord,
whose confidence is in him.
He will be like a tree planted
by the water
that sends out its roots by
the stream.
It does not fear when heat
comes;
its leaves are always green.
It has no worries in a year of
drought
and never fails to bear
fruit.

Jeremiah 17:7-8

TABLE OF CONTENTS

CHAPTER 1. GENERAL INTRODUCTION

General Overview

A variety of metalloproteins act as redox enzymes and electron carriers in respiration and photosynthesis, metabolism of nonmetals, and other biological processes.[1-5] Fundamental principles of biological reactivity can be understood only if interactions and reactions between proteins are understood on the molecular level. The biological redox-processes may require several steps including protein recognition and binding, protein rearrangement, and chemical transformations. A theoretical basis for what physical factors control the rate of long-range electron transfer is well known, so the kinetics of electron-transfer reactions can be used as a tool to explore dynamic processes that control overall biological reactions.[4,6]

We use kinetics of photoinduced redox reactions to study protein-protein recognition and configurational interconversion of a diprotein complex that may control the electron-transfer process. In this work we explore the interaction between the physiological partners cytochrome f and cytochrome c_6 from $C.$ $reinhardtii$.

Cytochrome f interchangeably reacts with cytochrome c_6 and plastocyanin, two proteins that have different structures and redox centers, but similar physico-chemical properties. Because cytochrome c_6 and plastocyanin must recognize the same physiological partners, these two proteins are expected to have similar surface patterns.[7] But the question remains, how do aforementioned differences and similarities reflect on protein docking and dynamics of the diprotein complex. Extensive data on the reaction between cytochrome f and plastocyanin already exist, which allowed us a comparison of cytochrome c_6 and plastocyanin in their corresponding reactions with their common partner.[7,8]

To learn about protein-protein recognition and dynamics of electron transfer between proteins, we used various experimental techniques such as laser flash photolysis, chemical cross-linking, and optical spectroscopy. Since both cytochrome f and cytochrome c_6 are c-type cytochromes, their chromophores overlap and it is spectroscopically difficult to study any simultaneous change of their redox states. We surmount this difficulty by replacing the iron ion in cytochrome c_6 with zinc(II). The photoexcitation of zinc cytochrome c_6 produces a long-lived triplet state that is a strong reducing agent. Direct photooxidation obviates the need for an external reducing agent, which makes interpretation of kinetics data more straightforward. Moreover, in the fast photoinduced reactions, the dynamic processes of interest that are often masked in the slow thermal reactions become detectable. We study the effects of ionic strength, solution viscosity, and temperature on the electron-transfer reaction between cytochrome f and cytochrome c_6.

Dissertation Organization

Chapter 2 explores the effects of ionic strength, solution viscosity, and chemical cross-linking on the protein-protein recognition and reaction between cytochrome f and cytochrome c_6. Chapter 3 is a comprehensive study of the temperature and solution viscosity effects on the mechanism of the electron-transfer reaction between cytochrome f and cytochrome c_6. In Chapter 4 we compare cytochrome c_6 and plastocyanin, with the emphasis on their reaction with cytochrome f. Recent theoretical studies emphasized the similarity between the docking configurations in cytochrome f/cytochrome c_6 and cytochrome f/plastocyanin complexes.[9] We derived from literature data and our own studies that the

energetics of configurational interconversion of the complex, rather than the initial configuration, will determine the mechanism of the electron-transfer reactions.

    Chapter 2 is a paper that has been published in a peer-refereed journal. Chapter 3 is a paper prepared for submission in a peer-refereed journal. Chapter 4 is a literature review complemented with and discussed in the context of results from chapters 2 and 3. Parts of Chapter 4 will be included in a future publication. The dissertation ends with Chapter 5, which gives the overall conclusions.

References

(1) Nocek, J. M.; Zhou, J. S.; Forest, S. D.; Priyadarshy, S.; Beratan, D. N.; Onuchic, J. N.; Hoffman, B. M. *Chemical Reviews (Washington, D. C.)* **1996**, *96*, 2459-2489.

(2) Liang, Z.-X.; Kurnikov, I. V.; Nocek, J. M.; Mauk, A. G.; Beratan, D. N.; Hoffman, B. M. *Journal of the American Chemical Society* **2004**, *126*, 2785-2798.

(3) Lasey, R. C.; Liu, L.; Zang, L.; Ogawa, M. Y. *Biochemistry* **2003**, *42*, 3904-3910.

(4) Davidson, V. L. *Accounts of Chemical Research* **2000**, *33*, 87-93.

(5) Crowley, P. B.; Ubbink, M. *Accounts of Chemical Research* **2003**, *36*, 723-730.

(6) Pletneva, E. V.; Fulton, D. B.; Kohzuma, T.; Kostić, N. M. *Journal of the American Chemical Society* **2000**, *122*, 1034-1046.

(7) Hervas, M.; Navarro, J. A.; De la Rosa, M. A. *Accounts of Chemical Research* **2003**, *36*, 798-805.

(8) Soriano, G. M.; Ponamarev, M. V.; Piskorowski, R. A.; Cramer, W. A. *Biochemistry* **1998**, *37*, 15120-15128.

(9) Gross, E. L.; Pearson, D. C., Jr. *Biophys J* **2003**, *85*, 2055-2068.

CHAPTER 2. METALLOPROTEIN ASSOCIATION, SELF-ASSOCIATION, AND DYNAMICS GOVERNED BY HYDROPHOBIC INTERACTIONS. SIMULTANEOUS OCCURRENCE OF GATED AND TRUE ELECTRON-TRANSFER REACTIONS BETWEEN CYTOCHROME F AND CYTOCHROME C_6 FROM CHLAMYDOMONAS REINHARDTII

Tijana Ž. Grove and Nenad M. Kostić

Department of Chemistry, Iowa State University, Ames, IA 50011, USA

All experiments, fittings, and interpretation of results were done by the primary author.

Abstract

Noninvasive reconstitution of the heme in cytochrome c_6 with zinc(II) ions allowed us to study the photoinduced electron-transfer reaction ^{3}Zncyt c_6 + cyt f (III) → Zncyt c_6^+ + cyt f (II) between physiological partners cytochrome c_6 and cytochrome f, both from *Chlamydomonas reinhardtii*. The reaction kinetics was analyzed in terms of protein docking and electron transfer. In contrast to various protein pairs studied before, both the unimolecular and the bimolecular mechanisms of this oxidative quenching takes place at all ionic strengths from 2.5 through 700 mM. The respective intracomplex rate constants are k_{uni} $(1.2 \pm 0.1) \times 10^4$ s^{-1} for persistent, and k_{bi} $(9 \pm 4) \times 10^2$ s^{-1} for the transient protein complex. The

former reaction seems to be true electron transfer, and the latter seems to be electron transfer gated by a structural rearrangement. Remarkably, these reactions occur simultaneously, and both rate constants are invariant with ionic strength. The association constant K_a for zinc cytochrome c_6 and cytochrome f(III) remains $(5 \pm 3) \times 10^5$ M^{-1} in the ionic strength range from 700 mM to 10 mM, and than rises slightly, to $(7 \pm 2) \times 10^6$ M^{-1}, as ionic strength is lowered to 2.5 mM. Evidently, docking of these proteins from *C. reinhardtii* is due to strong hydrophobic interaction slightly augmented by weak electrostatic attraction. Kinetics, chromatography, and cross-linking consistently show that cytochrome f self-dimerizes at ionic strengths of 200 mM and higher. Cytochrome f(III) does, but its dimer does not, quench triplet state ^{3}Zncyt c_6. Formation of this unreactive dimer is an important step in the mechanism of electron transfer. Not only association between the reacting proteins, but also their self-association, should be considered when analyzing reaction mechanisms.

Introduction

Because electron-transfer reactions between metalloproteins are essential to life it is important to understand their mechanisms. The overall redox process may consist of several steps, including protein-protein recognition, binding, and subsequent electron transfer.[1-3] Electrostatic and hydrophobic interaction govern the affinity and specifity in recognition and association.[4] Electrostatic interactions are well documented,[5-15] but mechanism and dynamics of electrostatic association are little understood. In simple cases there is only one energetically favorable binding configuration, which is also the reactive configuration. In more interesting cases an orientation that is optimal for binding is not optimal for electron

transfer or there are multiple binding conformations with similar energy, only some of which are competent for electron transfer. [16]

Very recent studies have shown that hydrophobic interaction can additionally stabilize the electrostatic complex. [4,17-22] Although hydrophobic interactions are expected to be prominent at physiological conditions (ionic strength of chloroplast interior is estimated at 400 mM) evidence that redox metalloproteins associate solely by hydrophobic interaction is scarce. Here we study the unexplored electron-transfer reaction of cytochrome f and reconstituted cytochrome c_6, and document the importance of hydrophobic forces not only for protein docking, but also for their reactivity.

Cytochrome f is the lumen-exposed part of the cytochrome $b_6 f$ complex. Its iron(III) form donates an electron to plastocyanin(II) (in plants and photosynthetic bacteria) or cytochrome c_6(III) (in cyanobacteria and some eucariotic algae), the reduced form of which then reduces the cofactor P700$^+$ of photosystem I. [5,6,23,24]

Some algae and cyanobacteria synthesize plastocyanin or cytochrome c_6. Others produce either protein, depending on the (un)availability of copper ions in the growth medium. [25,26] The notion that plastocyanin replaced cytochrome c_6 in the higher plants and some algae has very recently been refuted when cytochrome c_6 was found in a higher plant. [27] Although plastocyanin and cytochrome c_6 are functionally equivalent electron carriers, their primary, secondary, and tertiary structures are completely different. These proteins, however, have similar distribution of acidic patches and hydrophobic surfaces. [25] How these differences and similarities influence the mechanisms by which these proteins oxidize the same partner, cytochrome f(II), remains unknown. Electron-transfer reaction between cytochrome f and plastocyanin [5-7,14,17,24,28] *in vitro* involves electrostatic attraction between

the positively charged patch of lysine residues in the former protein and the negatively charged patch of acidic residues in the latter. [6-8,28,29]

Very little is known about the electron-transfer reaction between cytochrome f and cytochrome c_6. Ours is the first study of protein-protein interactions that govern the kinetics of electron transfer between them. Because both of them are heme proteins, whose absorption spectra overlap, it is almost impossible to follow spectroscopically the simultaneous oxidation of one heme group and reduction of the other. [30] In this study we overcame this difficulty by reconstituting cytochrome c_6 with zinc(II) ions and making the electron-transfer step photoinduced. Similar reconstitution of other cytochromes of type c does not perturb their conformation and interaction with their redox partners. [31,32] Although the photoinduced electron-transfer step in eq 1, which is followed by the reaction in eq 2 is not biological, the very high rate of this step allowed us to observe and quantify the association of proteins from the same organism, a process of great importance. Because the excited-state reaction in eq 1 and the subsequent ground-state reaction in eq 2 do not require any redox agents other than the interacting proteins, their association is not perturbed. Monitoring the electron-transfer reaction in eq 1 is our means of studying structural and dynamic aspects of metalloprotein association.

$$^3\text{Zncyt } c_6 + \text{cyt } f(\text{III}) \longrightarrow \text{Zncyt } c_6^+ + \text{cyt } f(\text{II}) \qquad (1)$$

$$\text{Zncyt } c_6^+ + \text{cyt } f(\text{II}) \longrightarrow \text{Zncyt } c_6 + \text{cyt } f(\text{III}) \qquad (2)$$
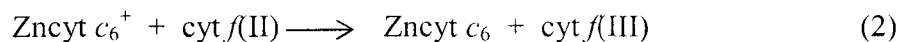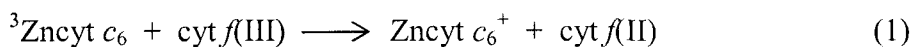
The results of this study are interesting and surprising. Cytochrome f from *Chlamydomonas reinhardtii* strongly associates not only with its physiological partner cytochrome c_6 but also with itself. The "cross"-association is driven predominantly, and the self-association entirely, by hydrophobic interaction. Self-association has been recognized as

an important means of regulating enzymatic reactions. [33-38] To our knowledge, this is the first report of self-association affecting the kinetics of electron-transfer reaction.

Previous research in our and other laboratories showed that mobility within the diprotein complex is necessary for efficient electron transfer as in eq 1. [39] Dynamics of electrostatic diprotein complexes has been studied in detail, [2,9,39-47] but that of non-electrostatic complexes has not, until now.

Materials and Methods

Chemicals and Buffers. Distilled water was demineralized to a resistivity greater than 17 MΩ cm by a Barnstead Nanopure II apparatus. Chromatographic resins and gels were purchased from Sigma Chemical Co; hydrogen fluoride, from Matheson Gas Product Inc; nitrogen and ultrapure argon, from Air Products Co; BCA protein assay reagent kit, from Pierce Co; all other chemicals, from Fisher Chemical Co. All buffers were prepared from the solid salts $NaH_2PO_4 \bullet H_2O$ and $Na_2HPO_4 \bullet 7H_2O$, and had pH of 7.00±0.05. For kinetic measurements the ionic strengths higher than 10 mM were adjusted with solid NaCl and for chromatography buffers of particular concentration were made. Unless concentration is stated, the buffers are specified by their ionic strength.

Proteins. Cytochrome f from *C. reinhardtii,* expressed from *E. coli*, was isolated and purified as described previously, [48] and was kindly provided by Professor William A. Cramer. Cytochrome c_6 from *C. reinhardtii* was isolated and purified by the published method. [25] Iron was removed, and the free-base protein was reconstituted with zinc(II) ions, by a modification of the standard procedure (manuscript in preparation). Zinc cytochrome c_6 was always kept in the dark. Concentrations of the two proteins were determined from their

UV-vis spectra, on the basis of known absorptivities: cytochrome f(II), $\Delta\varepsilon_{552}=26$ mM^{-1}cm^{-1}, cytochrome c_6(II), $\Delta\varepsilon_{552}=20$ mM^{-1}cm^{-1}, and zinc cytochrome c_6, $\Delta\varepsilon_{421}=(2.3\pm0.1)\times10^5$ M^{-1}cm^{-1}. The last value was determined from absorption spectra and quantification of total protein using the BCA protein assay reagent kit. All proteins were stored in liquid nitrogen. Before each series of experiments the buffer in protein stock solutions was replaced by the working buffer using so-called ultrafree-4 centrifugal filter obtained from Millipore Co.

Laser Flash Photolysis. Experiments were performed with the second harmonic (at 532 nm) of a Q-switched Nd-YAG laser, the instrument was described elsewhere. [49] Argon was passed first through water and then through the buffer solution. The required volume of buffer was deaerated in a 10-mm cuvette for at least 30 minutes before zinc cytochrome c_6 was added. After each addition of cytochrome f(III), the solution was gently deaerated for 10 to 15 minutes. In the titration experiments concentration of zinc cytochrome c_6 was kept constant in the interval 0.70-3.0 μM, and concentration of cytochrome f(III) was varied between 0.20 and 12 μM. Decay of the triplet state was monitored at 460 nm, where the transient absorbance reaches the maximum. The concentration of the triplet depended on the intensity of the laser pulse and was always much lower than the concentration of cytochrome f(III). Pseudo-first-order excess of cytochrome f(III) was maintained in all experiments. Formation and disappearance of the cation radical were monitored at 675 nm, where the difference between the absorbances of this species and the triplet is greatest. To enhance signal-to-noise ratio, at least 100 shots were collected and averaged.

Viscosity. The kinetic effects of viscosity were studied in the 10 mM sodium phosphate buffer at pH 7.0 and (20 ± 1) °C. Glycerol was added incrementally to the solution containing 3.0 μM zinc cytochrome c_6 and 9.0 μM cytochrome f(III), up to the concentration of 80 % w/v. The viscosity of the solution was determined from the tables. [50,51]

Cross-linking of Cytochrome f. A solution containing 5.0 μM cytochrome f and 50-fold molar excess of 1-[3-(dimethylamino)propyl]-3-ethylcarbodiimide hydrochloride (EDC) in sodium phosphate buffer at pH 7.0 and ionic strength 700 mM was stirred at room temperature. After 4 hours the reaction mixture was subjected to size-exclusion HPLC.

HPLC Separations. Hewlett Packard 1100 HPLC system contained an autosampler and a multiwavelength detector set to 215, 280, and 410 nm. Absorption at 215 nm is common to all peptides and proteins; that at 280 nm is due to aromatic residues; and that at 410 nm is diagnostic of heme. In the reverse-phase separations, an analytical Vydac C5 column 214TP54 (sized 150 x 4.6 mm, beads of 5 μm) was used. The eluting solvent A was 0.10% (v/v) trifluoroacidic acid in H_2O, and solvent B was 0.08% (v/v) trifluoroacidic acid in acetonitrile. In a typical run, the percentage of solvent B in the eluent was kept at 0% for 5 min after the injection of the sample, and then raised gradually to 45% over a 35-min period. The flow rate was 1.0 mL/min.

The size-exclusion separations were made with a Superdex 75 HR 10/30 column, having optimal separation range from 3 to 70 D. The solvent was a 100 mM (concentration) phosphate buffer, and the flow rate was 0.50 mL/min. The size-exclusion column was calibrated with bovine serum albumine (67 D), ovalbumin (43 D), carbonic anhydrase (29 D), trypsin inhibitor (20 D), and myoglobin (17 D). The void volume of the column was determined using blue dextran 2000. In size-exclusion separations the protein concentration was varied between 2.0×10^{-6} and 2.0×10^{-5} M for cytochrome f, and between 1.0×10^{-6} and 5.0×10^{-5} M for cytochrome c_6.

Analytical Ultracentrifugation. Sedimentation equilibrium involved cytochrome c_6(II) dissolved in phosphate buffer having pH 7.0 and ionic strength 300 mM at room temperature. The protein concentration was varied from 2.0×10^{-6} to 8.0×10^{-6} M. A Beckman

Optima XL-A analytical ultracentrifuge equipped with an An60-Ti rotor ran at 30 000 rpm. Absorbance detector was set at 410 or 550 nm, depending on protein concentration, so that absorbance stayed below 0.7. Data were collected at a spacing of 1.0×10^{-3} cm, with ten averages, in a step-scan mode every 3 hours. Equilibrium was reached when the absorbance stopped changing. The molecular mass of monomeric cytochrome c_6 was set to the value obtained from amino acid sequence, 9.8 D.

Fittings of the Kinetic Data. The rate constants for the reaction in eq 1 were obtained from the analysis of the changes of absorbance at 460 and 675 nm with time. The former change corresponds to the decay of ^{3}Zncyt c_6 and is a sum of several exponential terms (eq 3). The latter change is caused by both the triplet and the cation radical and is described by eqs 4-7. [52] Contribution of the triplet to the absorbance change at 675 nm is given by eq 5, in which a_t is the instantaneous absorbance after the laser flash. The contribution of cation radical is fitted with eq 7.

$$\Delta A_{460} = \sum_i a_i \exp(-k_i t) + b \tag{3}$$

$$\Delta A_{675} = \Delta A_{\text{triplet}} + \Delta A_{\text{cation}} \tag{4}$$

$$\Delta A_{\text{triplet}} = a_t \left[\sum_i f_i \exp(-k_i t) \right] \tag{5}$$

$$f_i = a_i / (a_{\text{uni}} + a_{\text{bi}}) \quad i = \text{uni, bi} \tag{6}$$

$$\Delta A_{\text{cation}} = a_c \left[\exp(-k_{fall} t) - \exp(-k_{rise} t) \right] \tag{7}$$

Kinetic results were analyzed with the SigmaPlot v.5.0, from SPSS Inc. The error margins for all rate constants (k) and amplitudes (a) obtained from the fitting of the transient-absorbance changes include two standard deviations, i. e., correspond to the confidence limit of 95 %. In some plots error bars for some of the points are large, but fortunately these points are not crucial for the fitting and do not alter the results and their discussion. Dependence of the observed rate constant, k_{obs}, for the slower phase on the concentration of free cytochrome

f(III) was fitted with the improved steady-state equation (eq 8), [53] in tandem with eq 9, as in several previous studies from this laboratory. [12,20,43,54]

$$k_{obs} = \frac{k_{on}\,k_{bi}\,[\text{cyt}\,f(\text{III})]}{k_{off} + k_{bi} + k_{on}\,[\text{cyt}\,f(\text{III})]} \qquad (8)$$

$$[\text{cyt}\,f(\text{III})] = [\text{cyt}\,f(\text{III})]_0 - 0.5\{[\text{Zncyt}\,c_6]_{tot} + [\text{cyt}\,f(\text{III})]_0 + K_a^{-1} - \qquad (9)$$
$$((([\text{Zncyt}\,c_6]_{tot} + [\text{cyt}\,f(\text{III})]_0 + K_a^{-1})^2 - 4[\text{Zncyt}\,c_6]_{tot}[\text{cyt}\,f(\text{III})]_0)^{0.5}\}$$

Many attempts to obtain the association constant K_a from fitting experimental results to eq 8 with SigmaPlot software failed, because a global minimum and several local minima of the sum of squares occurred with similar probabilities. Each of these occurrences yielded a different set of fitting parameters k_{on} and k_{off}, the ratio of which is K_a. Unfortunately, methods of numerical analysis often fail when data are fitted to an equation that contains a product of a very small and very large number. A common case in kinetics is a product between

ncentration and rate constant, such as $k_{on}[\text{cyt}\,f(\text{III})]$ in eq 8. Rescaling equation parameters sometimes improves numerical behavior and produces reasonable fittings. The occurrence of the "multiple minima" is not yet adequately addressed in SigmaPlot, but we managed to avoid this problem. We designed our experiments so that complex kinetic equations, ambiguous fittings, and analysis of possibly unreliable fitting parameters became unnecessary. The rate constants k_{uni} and k_{bi} were read directly from the plots in Figures 2 and 3, and the association constant K_a was obtained from the fractional contributions (eq 6) of the persistent (a_{uni}) and the transient (a_{bi}) complex to the transient-absorbance change using eqs 10 and 11, which are explained elsewhere.[52,77]

$$f_{uni} = \frac{1}{2[\text{Zncyt}\,c_6]}\{[\text{Zncyt}\,c_6] + [\text{cyt}\,f(\text{III})] + 1/K_a - ([\text{Zncyt}\,c_6] + [\text{cyt}\,f(\text{III})] + 1/K_a)^2 \qquad (10)$$
$$- 4[\text{Zncyt}\,c_6][\text{cyt}\,f(\text{III})])^{0.5}\}$$

$$\frac{[\text{cyt} f(\text{III})]}{f_{\text{uni}}} = \frac{[\text{cyt} f(\text{III})]}{g} + \frac{1}{gK_{\text{a}}} \qquad (11)$$

Results

Natural Decay of the Triplet State ^{3}Zncyt c_6. In the absence of a quencher, the

natural decay of the triplet excited state of the porphyrin to its ground state is

monoexponential (eq 12). The rate constant, k_{nd}, is 100 ± 10 s^{-1} at room temperature in

phosphate buffer having pH 7.00 and is independent of protein concentration in the interval

from 1.0 to 10 μM and of ionic strength in the interval from 2.5 to 700 mM.

$$\Delta A_{460} = a_{\text{nd}} \exp(-k_{\text{nd}}t) + b \qquad (12)$$

Oxidative Quenching of the Triplet State ^{3}Zncyt c_6 by Cytochrome f(III) is

Biphasic at All Ionic Strengths. In the presence of cytochrome f(III), decay of the triplet is

accelerated and is best described by a biexponential function (eq 13 and Figure 1a) at all

tested ionic strengths, from 2.5 through 700 mM. The rate constant k_{uni}, for the faster of the

two phases, is independent of concentration of cytochrome f(III) and ionic strength, as Figure

2 shows. The rate constant k_{obs}, for the slower phase, levels off at relatively high cytochrome

f(III) concentrations. As ionic strength is raised, the approximate breaking point in the plots

shifts towards higher ratios of the protein concentrations cyt f(III)/Zncyt c_6, that is, to a

higher concentration of the cytochrome f(III); see Figure 3. The rate constants for the faster

(k_{uni}) and slower (k_{bi}) phase of the quenching reactions are listed in Table 1. The rate

constants for the

$$\Delta A_{460} = a_1 \exp(-k_{\text{uni}}t) + a_2 \exp(-k_{\text{bi}}t) + b \qquad (13)$$

appearance and disappearance of the cation radical, shown in Figure 1b, are independent of

the cytochrome f(III) concentration. The absorbance at 675 nm grows at the rate of

$(5.6\pm0.6)\times10^4\,s^{-1}$ and declines at the rate of $(1.3\pm0.1)\times10^4\,s^{-1}$. This latter rate constant is the same as the k_{uni}. The increase in the absorbance at 675 nm is due to the back reaction (eq 2), and its decrease is due to the forward reaction (eq 1). [20,51] This study concerns the forward reaction because this reaction gives the information about protein association.

Kinetic Effects of Viscosity. The reaction in eq 1 was studied at ionic strength of 10 mM and temperature 20 ± 1 °C. The decay of ^{3}Zncyt c_6 remains biphasic throughout the viscosity range studied, from 1.005 through 60.1 cp. The amplitudes of both phases are unaffected by viscosity, as Figure 4 shows. Figure 5 shows that the rate constant for unimolecular quenching, k_{uni}, does not depend on viscosity, but the rate constant for the bimolecular quenching, k_{bi}, does.

Evidence that Cytochrome c_6 is Monomeric. In analytical centrifugation experiments, as the concentration of the protein is raised, the observed molecular mass stays constant and equal to that

calculated from amino-acid sequence, as Figure S4 shows. In size-exclusion HPLC experiments, the elution time of 26 min corresponds to the molecular mass of the monomer; see Figure S5.

Evidence for the Dimerization of Cytochrome f. Size-exclusion HPLC of cytochrome f solutions at ionic strengths 200 mM and higher shows an unsymmetric signal that is broadened on the side of shorter elution times. Repeated chromatography of the main fraction, having elution time of 21 min, and of the shoulder preceding it yielded the same chromatogram: the main band at 21 min and a broad shoulder at shorter times, as shown in Figure 6a. The UV-vis spectra of the main and shoulder fractions are identical to each other and to the spectrum of cytochrome f prior to the separation. The main fraction and the shoulder fraction separated by size gave the same reverse-phase chromatograms, shown in

Figure 6b, consisting of one single, sharp, symmetrical signal.Cross-linking of Cytochrome *f.*

Cross-linking of cytochrome *f* with the carbodiimide EDC yielded only two products, which

eluted from the size-exclusion HPLC column in 18 and 21 min. The ratio of their molecular

masses is 1.8, as Figure 7 shows. Evidently, the first and the second fraction, respectively,

are dimer and monomer of cytochrome *f.*

Attempt at Oxidative Quenching of ^{3}Zncyt c_6 with Dimer of Cytochrome *f*(III).

Attempts to oxidatively quench ^{3}Zncyt c_6 with the product of cross-linking gave kinetic

traces that were well fitted with the monoexponential function in eq 12. The rate constant

obtained from these fittings is 111 ± 1 s^{-1}, same as that for natural decay of the triplet state.

Residuals of the fitting are presented in Figure S3 in the Supporting Information.

Discussion

Interactions Between Metalloproteins. Our research group extensively studied the

mechanism of electron-transfer reaction and dynamic aspects of docking between zinc

cytochrome *c* and plastocyanin. [12,13,20,39-44,51,52,56-58] In this and similar systems,[59-63] where

proteins have high association constants, the kinetics is biphasic at low ionic strength. At

intermediate and high ionic strength, kinetics is monophasic, and the observed rate constant

is directly proportional to the concentration of the reactant in excess. When the association

constant for a metalloprotein pair is low even at low ionic strength, the observed rate constant

linearly depends on concentration. [6,14,15,16,26,28,64-71] In some cases kinetics of interprotein

reaction may be monophasic throughout, because so called saturation occurs under different

reaction conditions.

In various protein pairs the rate constant for electron transfer and the association constant markedly decrease as ionic strength is raised because electrostatic attraction dominates protein-protein association. Hydrophobic interaction unaccompanied by electrostatic attraction, a phenomenon well-documented in enzyme-substrate binding,[34,72-74] has only begun to be noticed in association of redox proteins.[19,21,22,26] Cytochrome f and plastocyanin from *Phormidium laminosum* reportedly are held mostly by hydrophobic forces.[4,75]

Cytochrome f and Cytochrome c_6. The water-soluble part of cytochrome f from *C. reinhardtii* is an elongated, β-barell protein, the iron(III) form of which has a net charge of -2 at pH of 7.0 (assuming normal pK_a values). Because the crystal structure of the membrane-bound cytochrome $b_6 f$ complex is unknown, nearly all kinetic studies *in vitro* have been done with the truncated form of cytochrome f.[23] A cationic patch of lysine residues has been implicated in docking with plastocyanin.[6,7,14,28] The biological function of the hydrophobic outer face of the heme-binding pocket in cytochrome f, however, has barely been studied.[17] We are interested in this hydrophobic area because both acidic substituents (so-called propionate chains) and one of the vinyl substituents of the heme are accessible in this part of the protein surface, as shown in Figure 8a.

Cytochrome c_6(II) from *C. reinhardtii* has net charge -7 at pH 7.0 (assuming normal pK_a values). As Figure 8a shows, the heme is largely buried in the protein; only one carboxylic group and a porphyrin edge are exposed. The surface around these exposed parts is largely nonpolar, except for Lys29, Lys57, and Asp41 residues.[25] Anionic groups are mostly located on the opposite side from the exposed parts of the heme.[76]

On the basis of the NMR spectroscopic experiments it was vaguely suggested that electron-transfer reactions involving cytochrome f, cytochrome c_6, and plastocyanin may

occur by different mechanisms, depending on the organism to which these proteins belong. [21] We test this proposition by studying the reactions between homologous proteins, those belonging to the same organism.

Mechanism of ^{3}Zncyt c_6 Quenching by Cytochrome f. The excited state of zinc porphyrin, ^{3}Zncyt c_6, produced by a laser flash, is oxidatively quenched by cytochrome f(III) according to eq 1. The resulting cation radical, Zncyt c_6^+, returns to the initial ground state in a thermal back reaction shown in eq 2. This study deals with the photoinduced reaction in eq 1. Unexpectedly, this reaction is biphasic at all ionic strengths examined, not only at low ionic strength, as was the case in numerous studies cited above. (See Scheme 1.) The intramolecular rate constant, k_{uni}, for the faster phase does not depend on the cytochrome f(III) concentration and ionic strength. Its values, given in Table 1, are read directly from the horizontal plots in Figure 2. The relative amplitude of this phase (f_{uni}) increases with the concentration of the persistent complex as the cytochrome f(III) concentration is raised, as shown in Figure S1. This rate constant corresponds to the intracomplex reaction within the persistent diprotein complex Zncyt c_6/cyt f(III), which already exists in solution before the laser flash. The observed rate constant for the slower phase, k_{obs}, does depend on cytochrome f(III) concentration. Because this phase is the bimolecular reaction between free proteins that associate in a transient Zncyt c_6/cyt f(III) complex, the plateau in Figure 3 corresponds to the maximal value of k_{obs}, achieved when zinc cytochrome c_6 is completely associated with cytochrome f(III). Therefore, the intracomplex rate constant k_{bi}, for the transient diprotein complex, can be read from the leveled plot. Despite the large error bars for some of the points in Figure 3, the k_{bi} values are sufficiently precise for our discussion; these results also are given in Table 1. Direct detection of the cation radical Zncyt c_6^+ at both low and high ionic strength is evidence that quenching occurs by oxidation of the triplet state.

Association Between Cytochrome f and Cytochrome c_6 from *C. reinhardtii* is Due Mostly to Hydrophobic Interaction. The persistence of the two kinetic phases of the reaction in eq 1 at ionic strength as high as 700 mM is evidence that electrostatic attraction plays a small, if any, role in association of these two proteins. We determined the association constants directly form the amplitudes of the two phases shown in Figures 2 and 3, using eqs 10 and 11.[52,77] (Fitting of the amplitudes is shown in Figures S1 and S2 in Supporting Information.) In this treatment only the total concentration of cytochrome f(III) matters, and its state (free or bound) does not matter. These two straightforward methods are independent of the mechanism of the subsequent electron transfer. Indeed, as Table 1 shows, fittings to eqs 10 and 11 gave consistent results. Invariance of k_{uni}, k_{bi}, and K_a with ionic strength consistently shows that the interaction between cytochrome c_6 and cytochrome f is not electrostatic. Indeed, hydrophobic interaction is fully consistent with Figure 8b, which shows hydrophobic surfaces surrounding the exposed parts of the heme in both proteins. Further speculation about structural and other detailes of this complex is unwarranted. As Table 1 shows, the association constant K_a decreases a little when ionic strength is raised from 2.5 to 10 mM and stays almost unchanged at higher ionic strengths. This initial drop is a sign of weak electrostatic attraction, which augments the strong hydrophobic effect insensitive to ionic strength. This weak electrostatic interaction cannot be atributed to the net charges of cytochrome c_6(II) and cytochrome f(III), which are −7 and −2 at pH 7.0, respectively; local charges are relevant here. Indeed, Ullmann et al. identified a minor anionic (acidic) patch in cytochrome c_6 that may interact with the predominant cationic (basic) patch of lysine residues in cytochrome f;[55] these patches are shown in Figure 8c. This pair of redox metalloproteins is remarkable because association is dominated by hydrophobic interactions and only weakly enhanced by electrostatic interactions.

Multiple Configurations of Diprotein Complexes in General. Much evidence

shows that the same pair of redox proteins may form multiple complexes, but little

experimental evidence shows that these complexes may undergo essentially the same

intracomplex electron-transfer reaction at different rates. This last notion is plausible and has

been accepted even though experimental studies corroborating it are still few. Three recent

studies have uniformly dealt with photoinduced reactions in which the triplet excited state of

zinc cytochrome c is oxidatively quenched by heme proteins or a metal complex. Two

simultaneous first-order reactions are detected in each case, but more than two complexes

may perhaps be present. [45,46,51,78-83] The variety of kinetic results in these three studies shows

the diversity of dynamic properties of fairly similar donor-acceptor systems, all of which are

mostly held by electrostatic forces. No two of these systems show the same effects and

noneffects of ionic strength and viscosity on the intracomplex rate constant. Clearly, general

rules about the dynamic aspects of electron-transfer reactions within protein complexes still

elude us.

Multiple Configurations of Diprotein Complexes of Zinc Cytochrome c_6 and

Cytochrome f. By monitoring the decay of the triplet state ^{3}Zncyt c_6 we detected the

persistent complex in Scheme 1, determined its association constant K_a, and precisely

determined its rate constant k_{uni}. We also detect the transient complex, and determine its rate

constant, k_{bi}, reliably but less precisely because kinetic traces due to the cation radical Zncyt

c_6^+ are relatively noisy. Fortunately, both rate constants are known with precision that is

sufficient for the discussion that follows.

I. Kinetic Noneffects of Ionic Strength – Evidence for Hydrophobic Interaction.

Table 1 shows that the intracomplex rate constants for the persistent (k_{uni}) and transient (k_{bi})

complexes in Scheme 1 differ as much as twentyfold and that both values are invariant with

ionic strength over a wide range. This invariance shows, for the first time, that hydrophobic, and not only electrostatic, interaction between metalloproteins can give rise to structurally heterogeneous association, which in turn gives rise to multiphasic reactivity.

II. Kinetic Noneffects and Effects of Viscosity – Evidence for Simultaneous Occurrence of True and Gated Electron Transfer. In previous studies in our laboratory, changing solution viscosity was used to determine whether the electron-transfer reaction is gated. [12,13,39,44,52] An increase in viscosity slows down protein motion and rearrangement of the diprotein complex, but does not affect association constant and the rate constants of the so-called true and coupled electron-transfer reactions. [52]

Glycerol is noninvasive to proteins and even stabilizes them. Because hydrophobic interactions are essential for protein folding, and glycerol does not unfold proteins, this solvent evidently does not perturb hydrophobic interaction. Indeed, relative amplitudes of the persistent and transient complex are unaffected by glycerol; see Figure 4. Therefore, the association constant K_a must also be unaffected.

Independence of the rate constant k_{uni} of solution viscosity, shown in Figure 5a, is evidence for true electron transfer within the persistent diprotein complex. Large and smooth dependence of the rate constant k_{bi} on solution viscosity, shown in Figure 5b, is diagnostic of gated electron transfer within the transient (collisional) diprotein complex. Electron transfer is the rate-limiting step in the unimolecular reaction because the persistent complex either is static or rearranges at a rate much higher than 1.2×10^4 s^{-1}, but the transient complex rearranges at a rate of $(9 \pm 4) \times 10^2$ s^{-1} (the average of the four values of k_{bi} in Table 1). Because this latter process is slower than the (unobservable) electron-transfer step within this complex, we detected this structural process when we monitored electron transfer that is controlled by it.

Self-association of Cytochrome *f*. Figure 3 shows that as the ionic strength is raised, a greater excess of cytochrome *f*(III) over zinc cytochrome c_6 is needed to reach a plateau in k_{obs}. The cyt *f*(III)/Zncyt c_6 ratio at the onset of the plateau increases from 1.2 to ca. 2.7. Not all of cytochrome *f*(III) put in solution seems available for association (and subsequent reaction) with cytochrome c_6. The asymmetric chromatogram of cytochrome *f* in Figure 6a shows a main signal and a prominent shoulder on the side corresponding to a larger molecular mass. Repeated experiments with separate samples taken from the main fraction and from the incompletely-resolved fraction preceding it consistently yielded this same pattern, shown in Figure 6a. The width of the shoulder precluded accurate determination of the elution time of the aggregate and of its molecular mass, but we estimated its mass to be approximately twice the nominal value. Cytochrome *f*, and also each of its two incompletely separated fractions in Figure 6a, all consistently gave the same narrow and rather symmetric chromatogram in Figure 6b.

The size-exclusion pattern in Figure 6a is characteristic of self-association equilibrium that is fast on the chromatography time scale of minutes.[84] The reverse-phase pattern in Figure 6b, however, proves that both fractions in Figure 6a contain the same protein – cytochrome *f*. If those fractions had contained different proteins of similar molecular masses, these proteins would have eluted separately. This did not happen. Instead, when all noncovalent interactions between the cytochrome *f* molecules were disrupted by denaturation, in the reverse phase experiment, the sample became homogeneous in terms of polarity.

Covalent cross-linking followed by size-exclusion chromatography is the standard method for detecting protein association.[85] An existing oligomer is captured by specific cross-linking, and a distinct signal appears in the chromatogram.[33,85,86] Random cross-

linking gives a multitude of chromatographic features, which may be smeared. [85] As Figure 7

shows, cytochrome f gave one distinct new fraction, whose molecular mass is approximately

twice that of the protein (monomer). Although EDC was present in large excess over the

protein, higher oligomers were absent. Evidently, cross-linking captures a dimer that already

exists in solution. Because at the ionic strength of 700 mM all electrostatic interactions are

absent, we conclude that the protein dimer is held by hydrophobic forces.

Kinetic Consequences of Cytochrome f Dimerization. As Figure 9 shows,

monomerric cytochrome f(III) does, but the cross-linked dimer of cytochrome f(III) does not,

quench the triplet state ^{3}Zncyt c_6. The observed rate constant in the latter case is that for the

natural decay of the triplet. Because the cytochrome f dimer is formed owing to hydrophobic

interactions (and is only reinforced by cross-linking), the protein molecules likely cover each

other's nonpolar surfaces (Figure 8b), and the heme edge is no longer accessible to zinc

cytochrome c_6.

Attempts to fit the results in Figure 3 to Scheme 1 with an improved steady-state

approximation (eq 8) failed. This fitting method, which had succeeded in treatments of other

diprotein complexes that associate and react by parallel unimolecular and bimolecular

mechanism, [12,13,51,56,61] is inaplicable to cytochrome c_6 and cytochrome f. The mechanism

involving only association between the reactants (i.e., Scheme 1 alone) proved to be

inadequate.

When our size-exclusion and reverse-phase HPLC separations and cross-linking

experiments (discussed above) clearly showed that cytochrome f forms a homodimer in

solution, we had to add the

$$2 \text{ cyt } f(\text{III}) \rightleftharpoons \text{ cyt } f(\text{III})/\text{cyt } f(\text{III}) \qquad (14)$$

equilibrium in eq 14 to Scheme 1. The fittings now become very good to excellent, as Figure 3 shows. The most surprising feature in Figure 3, namely the shifting of the "plateau point" to the increasing values of the [cyt f(III)]/[Zncyt c_6] ratio, was faithfully reproduced. This ratio is greater than unity not because larger hetero-oligomers of zinc cytochrome c_6 and cytochrome f(III) form but because a redox-inactive homodimer of cytochrome f(III) forms. As the concentration of this protein is raised, it increasingly associates not only with zinc cytochrome c_6, but also with itself, thus inhibiting the reaction in Scheme 1.

We can only conjecture about the significance *in vivo* of this process, which we documented *in vitro*. Dimerization of cytochrome f in the crystal has recently been considered. [23] The dimerization of cytochrome f from *C. reinhardtii* in aqueous solution is interesting because cytochrome b_6f is a dimer, but of unknown structure. [6,87-93] We detected dimerization at ionic strengths of both 300 and 700 mM, conditions relevant to the ionic strength *in vivo*, which is 300 mM. [24] We do not know of any other reports that kinetics of interprotein electron-transfer reaction is modulated by protein self-association and intend to study this mechanistic phenomenon and its possible biological ramifications.

Comparison of Cytochrome c_6 and Plastocyanin from *C. reinhardtii* in their Association and Electron Transfer with Cytochrome f from *C. reinhardtii*.

Chlamydomonas reinhardtii is the first organism known to biosynthesize both plastocyanin (when copper ions are available) and cytochrome c_6 (when they are unavailable) and to use either of these proteins as an electron carrier from cytochrome f(II) to P700$^+$ in photosystem I. [25] The reaction of each carrier with P700$^+$ is biphasic. Since the rate of the unimolecular process (the faster phase) is the same for copper(I) plastocyanin and cytochrome c_6(II), these two proteins probably interact similarly with photosystem I. [62] Association and reaction

between cytochrome f and plastocyanin have been much studied [4-8,14,17,18,22,24,26,29,55,94,95] but mostly with heterologous proteins. Their association is largely electrostatic. [5-8,14,26,29,55]

This study, however, showed that homologous proteins cytochrome f and cytochrome c_6 from *C. reinhardtii* associate by hydrophobic interactions. Although the persistent and transient complexes differ in reactivity, their different intracomplex rate constants are similarly invariant with ionic strength.

Conclusions

Photoinduced electron-transfer reactions are "clean" and fast, and therefore suitable for the study of protein association. Because electrostatic interactions are relatively easily detected and adjusted (by changing ionic strength), they have been much studied lately. Metalloprotein association, however, can be governed also by hydrophobic interactions, and resulting complexes can be as stable as typical electrostatic complexes. Persistent and transient complexes held by hydrophobic interactions differ so much in the interplay between electron-transfer step and configurational rearrangement that the intracomplex reaction is true electron transfer in the former and gated electron transfer in the latter. Remarkably, these reactions occur simultaneously in the same diprotein system. Not only association between electron donor and the electron acceptor, but also their self-association, should be kept in mind when analyzing complex reaction mechanism and finding unexpected kinetics.

Supporting Information Available: One figure showing the dependence of the relative amplitudes of the faster kinetic phase on cytochrome *f*(III) concentration; one figure showing the dependence of the ratio of cytochrome *f*(III) concentration and relative amplitude for the faster kinetic phase on the cytochrome *f*(III) concentration; one figure showing residuals for the fitting of traces in Figure 9 to the monoexponential function in eq 12, one figure showing the .dstudy of cytochrome c_6 by ultracentrifugation, and one figure showing size-exclusion chromatograms of cytochrome c_6. This material is available free of charge via the Internet at http://pubs.acs.org.

References

(1) Davidson, V. L. *Biochemistry* **2000**, *39*, 4924-4928.

(2) Davidson, V. L. *Accounts of Chemical Research* **2000**, *33*, 87-93.

(3) Davidson, V. L. *Biochemistry* **1996**, *35*, 14035-14039.

(4) Crowley, P. B.; Otting, G.; Schlarb-Ridley, B. G.; Canters, G. W.; Ubbink, M. *Journal of the American Chemical Society* **2001**, *123*, 10444-10453.

(5) Soriano, G. M.; Cramer, W. A.; Krishtalik, L. I. *Biophysical Journal* **1997**, *73*, 3265-3276.

(6) Soriano, G. M.; Ponamarev, M. V.; Piskorowski, R. A.; Cramer, W. A. *Biochemistry* **1998**, *37*, 15120-15128.

(7) Gong, X.-S.; Wen, J. Q.; Fisher, N. E.; Young, S.; Howe, C. J.; Bendall, D. S.; Gray, J. C. *European Journal of Biochemistry* **2000**, *267*, 3461-3468.

(8) Ubbink, M.; Ejdeback, M.; Karlsson, B. G.; Bendall, D. S. *Structure (London)* **1998**, *6*, 323-335.

(9) Liang, Z.-X.; Jiang, M.; Ning, Q.; Hoffman, B. M. *JBIC, Journal of Biological Inorganic Chemistry* **2002**, *7*, 580-588.

(10) Pletneva, E. V.; Laederach, A.; Kostić, N. M. *Abstr. Pap. - Am. Chem. Soc.* **2000**, *220th*, INOR-084.

(11) Sadeghi, S. J.; Valetti, F.; Cunha, C. A.; Romao, M. J.; Soares, C. M.; Gilardi, G. *JBIC, Journal of Biological Inorganic Chemistry* **2000**, *5*, 730-737.

(12) Crnogorac, M. M.; Shen, C.; Young, S.; Hansson, O.; Kostić, N. M. *Biochemistry* **1996**, *35*, 16465-16474.

(13) Ivkovic-Jensen, M. M.; Ullmann, G. M.; Young, S.; Hansson, O.; Crnogorac, M. M.; Ejdebaeck, M.; Kostić, N. M. *Biochemistry* **1998**, *37*, 9557-9569.

(14) Qin, L.; Kostić, N. M. *Biochemistry* **1993**, *32*, 6073-6080.

(15) Sokerina, E. V.; Ullmann, G. M.; Van Pouderoyen, G.; Canters, G. W.; Kostić, N. M. *JBIC, Journal of Biological Inorganic Chemistry* **1999**, *4*, 111-121.

(16) Liang, Z.-X.; Nocek, J. M.; Huang, K.; Hayes, R. T.; Kurnikov, I. V.; Beratan, D. N.; Hoffman, B. M. *Journal of the American Chemical Society* **2002**, *124*, 6849-6859.

(17) Gong, X.-S.; Wen, J. Q.; Gray, J. C. *European Journal of Biochemistry* **2000**, *267*, 1732-1742.

(18) Ejdebaeck, M.; Bergkvist, A.; Karlsson, B. G.; Ubbink, M. *Biochemistry* **2000**, *39*, 5022-5027.

(19) Cutruzzola, F.; Arese, M.; Ranghino, G.; van Pouderoyen, G.; Canters, G.; Brunori, M. *Journal of Inorganic Biochemistry* **2002**, *88*, 353-361.

(20) Zhou, J. S.; Kostić, N. M. *Journal of the American Chemical Society* **1991**, *113*, 6067-6073.

(21) Crowley, P. B.; Diaz-Quintana, A.; Molina-Heredia, F. P.; Nieto, P.; Sutter, M.; Haehnel, W.; De la Rosa, M. A.; Ubbink, M. *Journal of Biological Chemistry* **2002**, *277*, 48685-48689.

(22) Crowley, P. B.; Vintonenko, N.; Bullerjahn, G. S.; Ubbink, M. *Biochemistry* **2002**, *41*, 15698-15705.

(23) Chi, Y.-I.; Huang, L.-S.; Zhang, Z.; Fernandez-Velasco, J. G.; Berry, E. A. *Biochemistry* **2000**, *39*, 7689-7701.

(24) Soriano, G. M.; Ponamarev, M. V.; Tae, G. S.; Cramer, W. A. *Biochemistry* **1996**, *35*, 14590-14598.

(25) Kerfeld, C. A.; Anwar, H. P.; Interrante, R.; Merchant, S.; Yeates, T. O. *Journal of Molecular Biology* **1995**, *250*, 627-647.

(26) Schlarb-Ridley, B. G.; Bendall, D. S.; Howe, C. J. *Biochemistry* **2002**, *41*, 3279-3285.

(27) Gupta, R.; He, Z.; Luan, S. *Nature (London, United Kingdom)* **2002**, *417*, 567-571.

(28) Qin, L.; Kostić, N. M. *Biochemistry* **1992**, *31*, 5145-5150.

(29) Pearson, D. C., Jr.; Gross, E. L.; David, E. S. *Biophysical Journal* **1996**, *71*, 64-76.

(30) Navarro, J. A.; Hervas, M.; De la Rosa, M. A. *JBIC, Journal of Biological Inorganic Chemistry* **1997**, *2*, 11-22.

(31) Anni, H.; Vanderkooi, J. M.; Mayne, L. *Biochemistry* **1995**, *34*, 5744-5753.

(32) Ye, S.; Shen, C.; Cotton, T. M.; Kostić, N. M. *Journal of Inorganic Biochemistry* **1997**, *65*, 219-226.

(33) Dienys, G.; Sereikaite, J.; Luksa, V.; Jarutiene, O.; Mistiniene, E.; Bumelis, V.-A. *Bioconjugate Chemistry* **2000**, *11*, 646-651.

(34) Hornby, J. A. T.; Codreanu, S. G.; Armstrong, R. N.; Dirr, H. W. *Biochemistry* **2002**, *41*, 14238-14247.

(35) Lazazzera, B. A.; Bates, D. M.; Kiley, P. J. *Genes & Development* **1993**, *7*, 1993-2005.

(36) Moore, L. J.; Kiley, P. J. *Journal of Biological Chemistry* **2001**, *276*, 45744-45750.

(37) Silinski, P.; Allingham, M. J.; Fitzgerald, M. C. *Biochemistry* **2001**, *40*, 4493-4502.

(38) Silinski, P.; Fitzgerald, M. C. *Biochemistry* **2002**, *41*, 4480-4491.

(39) Zhou, J. S.; Kostić, N. M. *Journal of the American Chemical Society* **1993**, *115*, 10796-10804.

(40) Zhou, J. S.; Kostić, N. M. *Journal of the American Chemical Society* **1991**, *113*, 7040-7042.

(41) Zhou, J. S.; Kostić, N. M. *Journal of the American Chemical Society* **1992**, *114*, 3562-3563.

(42) Zhou, J. S.; Kostić, N. M. *Biochemistry* **1993**, *32*, 4539-4546.

(43) Ivkovic-Jensen, M. M.; Kostić, N. M. *Biochemistry* **1996**, *35*, 15095-15106.

(44) Ivkovic-Jensen, M. M.; Kostić, N. M. *Biochemistry* **1997**, *36*, 8135-8144.

(45) Lasey, R. C.; Liu, L.; Zang, L.; Ogawa, M. Y. *Biochemistry* **2003**, *42*, 3904-3910.

(46) Nocek, J. M.; Zhou, J. S.; Forest, S. D.; Priyadarshy, S.; Beratan, D. N.; Onuchic, J. N.; Hoffman, B. M. *Chemical Reviews (Washington, D. C.)* **1996**, *96*, 2459-2489.

(47) Walden, S. E.; Wheeler, R. A. *Journal of Physical Chemistry B* **2002**, *106*, 3001-3006.

(48) Soriano, G. M.; Guo, L.-W.; de Vitry, C.; Kallas, T.; Cramer, W. A. *Journal of Biological Chemistry* **2002**, *277*, 41865-41871.

(49) Pletneva, E. V.; Crnogorac, M. M.; Kostić, N. M. *Journal of the American Chemical Society* **2002**, *124*, 14342-14354.

(50) Weast, R. C.; Editor, Eds. *CRC Handbook of Chemistry and Physics. 68th Ed*, 1987.

(51) Pletneva, E. V.; Fulton, D. B.; Kohzuma, T.; Kostić, N. M. *Journal of the American Chemical Society* **2000**, *122*, 1034-1046.

(52) Ivkovic-Jensen, M. M.; Ullmann, G. M.; Crnogorac, M. M.; Ejdebaeck, M.; Young, S.; Hansson, O.; Kostić, N. M. *Biochemistry* **1999**, *38*, 1589-1597.

(53) Espenson, J. H. *Chemical Kinetics and Reaction Mechanisms*, 1995.

(54) Crnogorac, M. M.; Ullmann, G. M.; Kostić, N. M. *Journal of the American Chemical Society* **2001**, *123*, 10789-10798.

(55) Ullmann, G. M.; Hauswald, M.; Jensen, A.; Kostić, N. M.; Knapp, E.-W. *Biochemistry* **1997**, *36*, 16187-16196.

(56) Peerey, L. M.; Brothers, H. M., II; Hazzard, J. T.; Tollin, G.; Kostić, N. M. *Biochemistry* **1991**, *30*, 9297-9304.

(57) Zhou, J. S.; Brothers, H. M., II; Neddersen, J. P.; Peerey, L. M.; Cotton, T. M.; Kostić, N. M. *Bioconjugate Chemistry* **1992**, *3*, 382-390.

(58) Ivkovic-Jensen, M. M.; Yeung, S.; Hansson, O.; Kostić, N. M. *Book of Abstracts, 213th ACS National Meeting, San Francisco, April 13-17* **1997**, INOR-550.

(59) McLendon, G.; Miller, J. R. *Journal of the American Chemical Society* **1985**, *107*, 7811-7816.

(60) McLendon, G. *Accounts of Chemical Research* **1988**, *21*, 160-167.

(61) Qin, L.; Kostić, N. M. *Biochemistry* **1994**, *33*, 12592-12599.

(62) Hippler, M.; Drepper, F.; Farah, J.; Rochaix, J.-D. *Biochemistry* **1997**, *36*, 6343-6349.

(63) Hippler, M.; Drepper, F.; Haehnel, W.; Rochaix, J.-D. *Proceedings of the National Academy of Sciences of the United States of America* **1998**, *95*, 7339-7344.

(64) Furukawa, Y.; Ishimori, K.; Morishima, I. *Biochemistry* **2002**, *41*, 9824-9832.

(65) Liang, Z.-X.; Nocek, J. M.; Kurnikov, I. V.; Beratan, D. N.; Hoffman, B. M. *Journal of the American Chemical Society* **2000**, *122*, 3552-3553.

(66) Augustin, M. A.; Chapman, S. K.; Davies, D. M.; Sykes, A. G.; Speck, S. H.; Margoliash, E. *Journal of Biological Chemistry* **1983**, *258*, 6405-6409.

(67) Augustin, M. A.; Chapman, S. K.; Davies, D. M.; Watson, A. D.; Sykes, A. G. *Journal of Inorganic Biochemistry* **1984**, *20*, 281-289.

(68) Ahmad, I.; Cusanovich, M. A.; Tollin, G. *Biochemistry* **1982**, *21*, 3122-3128.

(69) Hazzard, J. T.; Rong, S. Y.; Tollin, G. *Biochemistry* **1991**, *30*, 213-222.

(70) Pan, L. P.; Hazzard, J. T.; Lin, J.; Tollin, G.; Chan, S. I. *Journal of the American Chemical Society* **1991**, *113*, 5908-5910.

(71) Hazzard, J. T.; Mauk, A. G.; Tollin, G. *Archives of Biochemistry and Biophysics* **1992**, *298*, 91-95.

(72) Jin, J.; Chang, J.; Stafford, D. W.; Straight, D. L. *Biochemistry* **2001**, *40*, 11405-11410.

(73) De Ferrari, G. V.; Canales, M. A.; Shin, I.; Weiner, L. M.; Silman, I.; Inestrosa, N. C. *Biochemistry* **2001**, *40*, 10447-10457.

(74) Fan, Y.-X.; McPhie, P.; Miles, E. W. *Biochemistry* **2000**, *39*, 4692-4703.

(75) Hart, S. E.; Schlarb-Ridley, B. G.; Delon, C.; Bendall, D. S.; Howe, C. J. *Biochemistry* **2003**, ACS ASAP.

(76) Dikiy, A.; Carpentier, W.; Vandenberghe, I.; Borsari, M.; Safarov, N.; Dikaya, E.; Van Beeumen, J.; Ciurli, S. *Biochemistry* **2002**, *41*, 14689-14699.

(77) Drepper, F.; Hippler, M.; Nitschke, W.; Haehnel, W. *Biochemistry* **1996**, *35*, 1282-1295.

(78) Mei, H.; Geren, L.; Miller, M. A.; Durham, B.; Millett, F. *Biochemistry* **2002**, *41*, 3968-3976.

(79) Leesch, V. W.; Bujons, J.; Mauk, A. G.; Hoffman, B. M. *Biochemistry* **2000**, *39*, 10132-10139.

(80) Mei, H.; Wang, K.; Peffer, N.; Weatherly, G.; Cohen, D. S.; Miller, M.; Pielak, G.; Durham, B.; Millett, F. *Biochemistry* **1999**, *38*, 6846-6854.

(81) Castro, G.; Boswell, C. A.; Northrup, S. H. *Journal of Biomolecular Structure & Dynamics* **1998**, *16*, 413-424.

(82) Zhou, J. S.; Tran, S. T.; McLendon, G.; Hoffman, B. M. *Journal of the American Chemical Society* **1997**, *119*, 269-277.

(83) Mei, H.; Wang, K.; McKee, S.; Wang, X.; Pielak, G. J.; Durham, B.; Millett, F. *Biochemistry* **1996**, *35*, 15800-15806.

(84) Dubin, P. L.; Editor, Eds. *Journal of Chromatography Library, Vol. 40: Aqueous Size-Exclusion Chromatography*, 1988.

(85) Loster, K.; Josic, D. *Journal of Chromatography. B, Biomedical Sciences and Applications* **1997**, *699*, 439-461.

(86) Schmid, B.; Einsle, O.; Chiu, H.-J.; Willing, A.; Yoshida, M.; Howard, J. B.; Rees, D. C. *Biochemistry* **2002**, *41*, 15557-15565.

(87) Soriano, G. M.; Ponamarev, M. V.; Carrell, C. J.; Xia, D.; Smith, J. L.; Cramer, W. A. *Journal of Bioenergetics and Biomembranes* **1999**, *31*, 201-213.

(88) Bron, P.; Lacapere, J.-J.; Breyton, C.; Mosser, G. *Journal of Molecular Biology* **1999**, *287*, 117-126.

(89) Cramer, W. A.; Soriano, G. M.; Zhang, H.; Ponamarev, M. V.; Smith, J. L. *Physiologia Plantarum* **1997**, *100*, 852-862.

(90) Poggese, C.; Polverino de Laureto, P.; Giacometti, G. M.; Rigoni, F.; Barbato, R. *FEBS Letters* **1997**, *414*, 585-589.

(91) Breyton, C.; Tribet, C.; Olive, J.; Dubacq, J.-P.; Popot, J.-L. *Journal of Biological Chemistry* **1997**, *272*, 21892-21900.

(92) Mosser, G.; Breyton, C.; Olofsson, A.; Popot, J.-L.; Rigaud, J.-L. *Journal of Biological Chemistry* **1997**, *272*, 20263-20268.

(93) Breyton, C.; Tribet, C.; Olive, J.; Recouvreur, M.; Popot, J.-L. *Photosynthesis: From Light to Biosphere, Proceedings of the International Photosynthesis Congress, 10th, Montpellier, Fr., Aug. 20-25, 1995* **1995**, *2*, 591-594.

(94) Morand, L. Z.; Frame, M. K.; Colvert, K. K.; Johnson, D. A.; Krogmann, D. W.; Davis, D. J. *Biochemistry* **1989**, *28*, 8039-8047.

(95) Ullmann, G. M.; Knapp, E.-W.; Kostić, N. M. *Journal of the American Chemical Society* **1997**, *119*, 42-52.

Table 1. Rate Constants Obtained from Fitting the Results in Figures 2 and 3 to the

Mechanism in Scheme 1 and eq 12, and Association Constants Obtained from

eqs 8 and 9

ionic strength, mM	$k_{uni}/10^4$ s^{-1} unimolecular mechanism	$k_{bi}/10^2$ s^{-1} bimolecular mechanism	$K_a/10^5$ M^{-1} from eq 8	$K_a/10^5$ M^{-1} from eq 9
2.5	1.1 ± 0.2	6.6 ± 0.2	70 ± 20	20 ± 10
10	1.3 ± 0.1	9 ± 2	4 ± 2	6 ± 2
300	1.2 ± 0.4	5.6 ± 0.2	4 ± 2	2 ± 1
700	1.1 ± 0.2	13 ± 5	8 ± 2	4 ± 2

Scheme 1. Mechanism of Electron Transfer

bimolecular
reaction

unimolecular
reaction

Zncyt c_6 + cyt f(III) $\xrightleftharpoons{K_a}$ Zncyt c_6/cyt f(III)

$h\nu \updownarrow k_{nd}$

^{3}Zncyt c_6 + cyt f(III)

$k_{on} \updownarrow k_{off}$

$h\nu \quad\quad k_{nd}$

transient
complex ^{3}Zncyt c_6/cyt f(III)

^{3}Zncyt c_6/cyt f(III) *persistent*
complex

k_{bi} $\quad$ k_{uni}

Zncyt c_6^{+}/cyt f(II)

k_{back}

Zncyt c_6/cyt f(III)
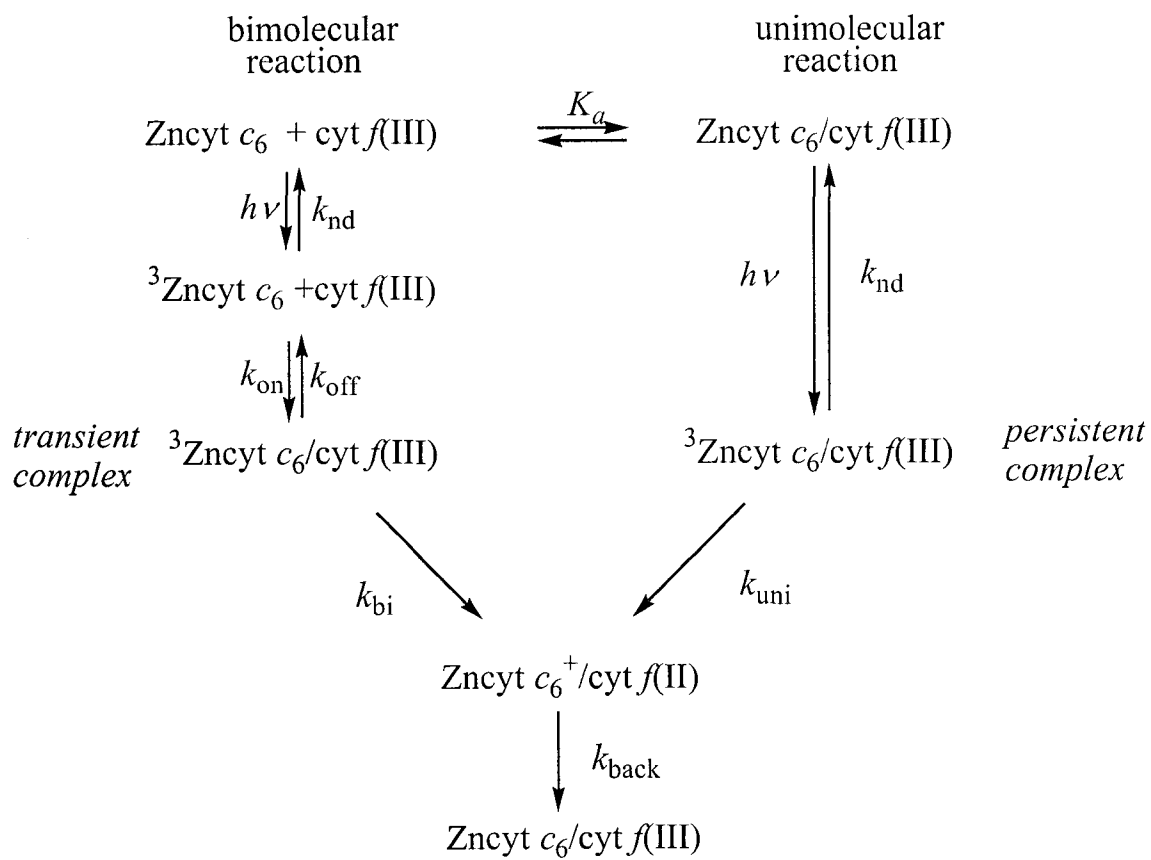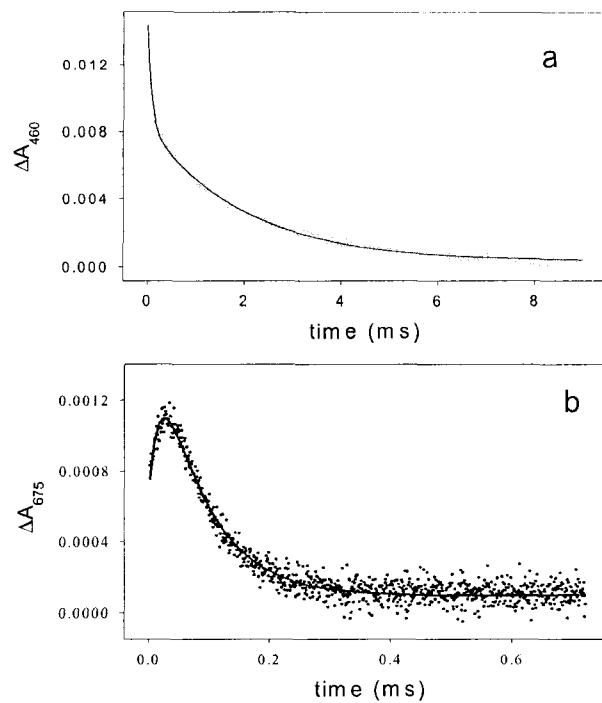
Figure 1. Transient-absorbance changes in a solution initially containing 3.0 µM zinc

cytochrome c_6 and 3.0 µM cytochrome f(III) in sodium phosphate buffer, at pH 7.0 and ionic

strength of 300 mM at room temperature. (a) Disappearance of the triplet state ^{3}Zncyt c_6

monitored at 460 nm. The line is a fitting to eq 13. (b) Formation and disappearance of the

cation radical Zncyt c_6^+ monitored at 675 nm. The line is a fitting to eqs 4-7.
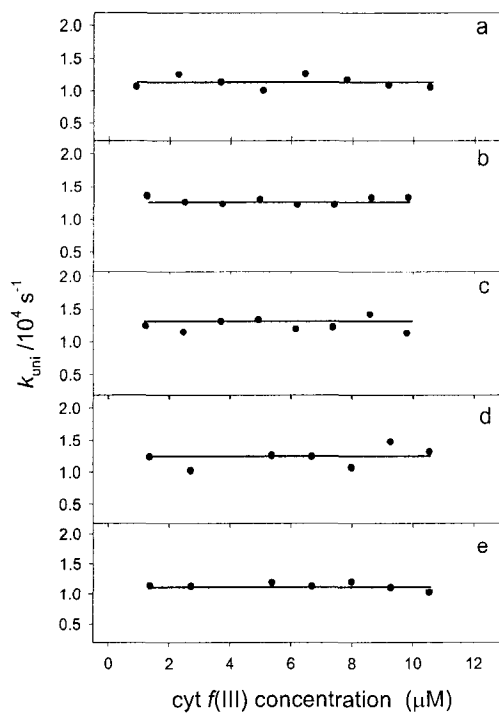
Figure 2. Independence of the microscopic rate constant k_{uni}, for the unimolecular

mechanism in Scheme 1, of the concentration of cytochrome f(III) in sodium phosphate

buffer at pH 7.0, room temperature, and ionic strength of (a) 2.5 mM, (b) 10 mM, (c) 100

mM, (d) 300 mM, and (e) 700 mM. The k_{uni} values are listed in Table 1. Error bars are

smaller than dots and invisible.
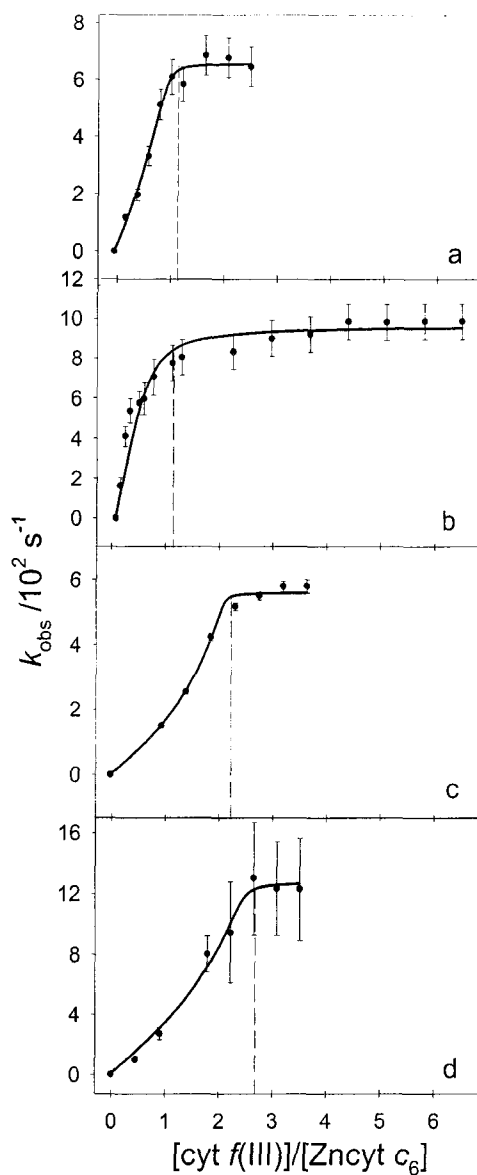
Figure 3. Dependence of the observed rate constant k_{obs} on the ratio of cyt f(III) and Zncyt c_6

concentrations, in sodium phosphate buffer at pH 7.0, room temperature, and ionic strengths

of (a) 2.5 mM, (b) 10 mM, (c) 300 mM, and (d) 700 mM. Note the shifting of the plateau

onset with rising ionic strength. Solid lines are fittings to the mechanism in Scheme 1 and eq

14. Error bars smaller than dots cannot be seen.
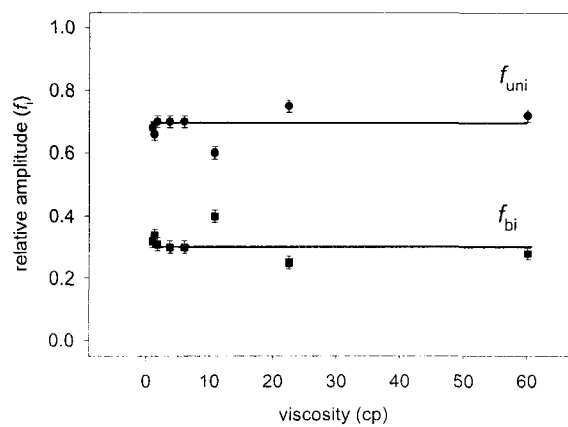
Figure 4. Independence of solution viscosity of the relative amplitudes f_{uni} and f_{bi},

respectively, of the unimolecular (•) and bimolecular (■) reaction in Scheme 1. Viscosity of

the sodium phosphate buffer solution at pH 7.0, ionic strength 10 mM, and 20±1 °C was

adjusted with glycerol.
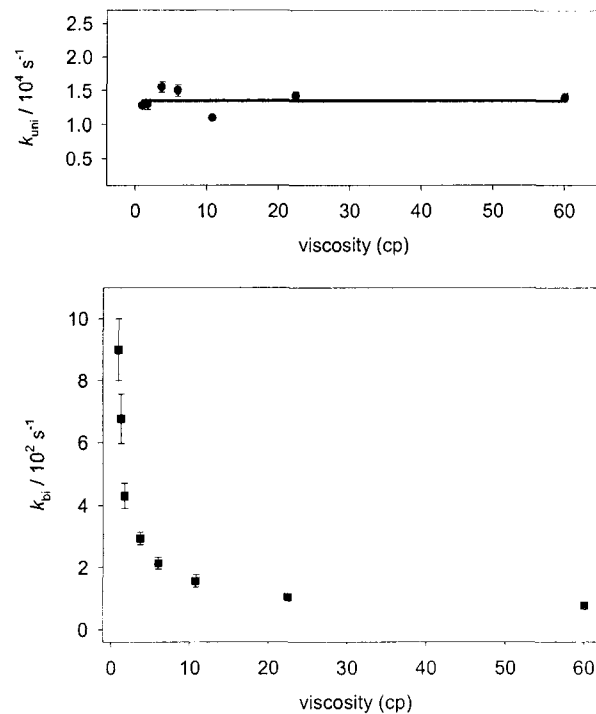
Figure 5. Dependence on the solution viscosity of the intracomplex rate constant for the (a)

unimolecular and (b) bimolecular reactions in Scheme 1. Viscosity of the sodium phosphate

buffer solution at pH 7.0, ionic strength 10 mM, and 20±1 °C was adjusted with glycerol.

Error bars smaller than dots cannot be seen.
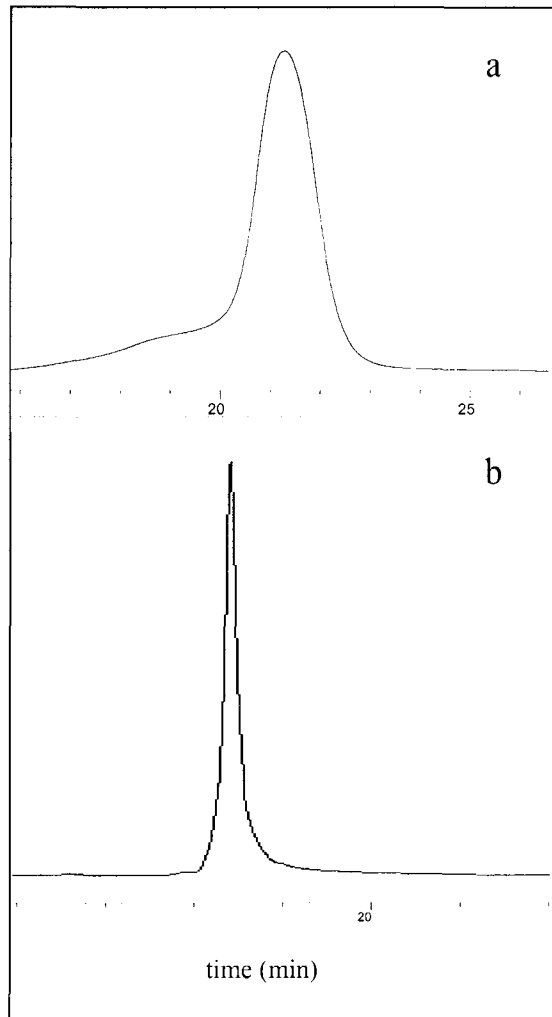
Figure 6. Chromatograms of a 5.0 μM cytochrome *f* from *C. reinhrdtii*. (a) Size-exclusion

HPLC, with a 100 mM (concentration) sodium phosphate buffer at pH 7.0. Note the shoulder

preceding the main signal. (b) Reverse-phase HPLC with 0.10% (v/v) trifluoroacidic acid in

water and 0.08% (v/v) trifluoroacidic acid in acetonitrile. Note the sharpness and symmetry

of the signal.

time (min)
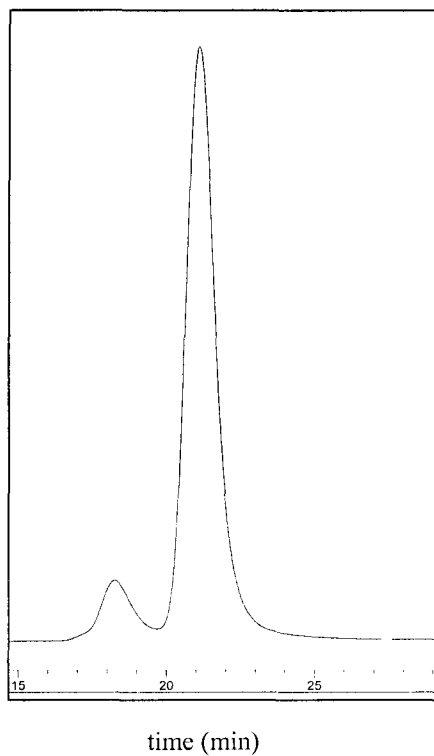
Figure 7. Size-exclusion HPL chromatogram of the reaction mixture containing cytochrome

f from *C. reinhardtii* and a large excess of carbodiimide EDC. Elution solvent is 100 mM

(concentration) sodium phosphate buffer at pH 7.0. The fractions eluting at 21.1 and 18.3

min are, respectively, cytochrome *f* and a cross-linked dimer of it.
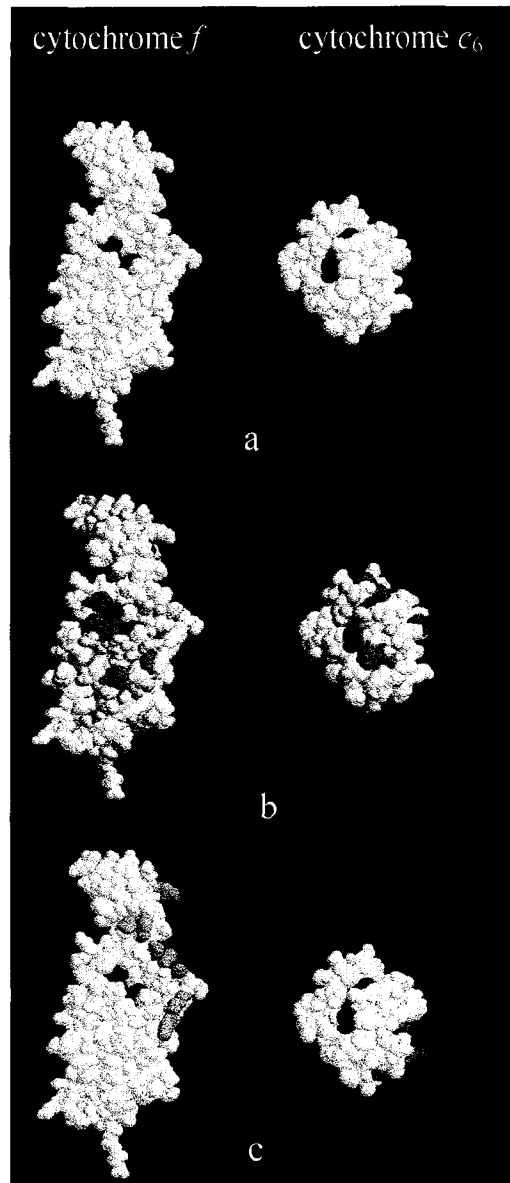
Figure 8. (a) Surfaces of (truncated) cytochrome *f* and cytochrome c_6 from *Chlamidomonas*

reinhartdtii. Color code: blue, basic residues; magenta, acidic residues; yellow, hydrophobic

residues; green, aromatic residues; and red, heme. (a) Exposed parts of the heme. (b)

Hydrophobic residues surrounding the exposed part of the heme, the proposed docking sites.

(c) Basic and acidic patch are assisting association through electrostatic attraction at low

ionic strength.
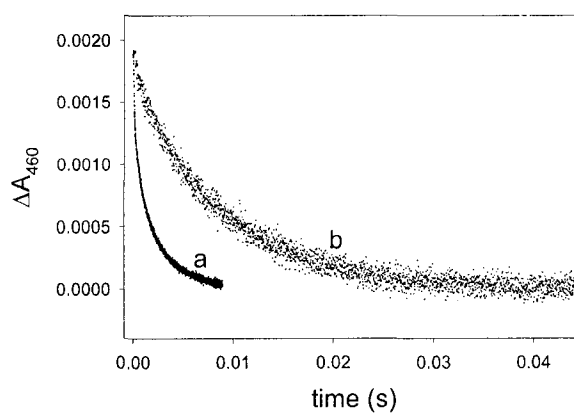
Figure 9. Disappearance of the triplet state ^{3}Zncyt c_6, monitored at 460 nm, in the solution

initially containing 3.0 μM zinc cytochrome c_6 and (a) 3.0 μM cytochrome f(III) or (b) 3.0

μM cross-linked dimer of cytochrome f(III). The solvent in both cases is a sodium phosphate

buffer at pH 7.00 and ionic strength of 300 mM. The triplet state is quenched in (a) but not in

(b).

Supporting Information
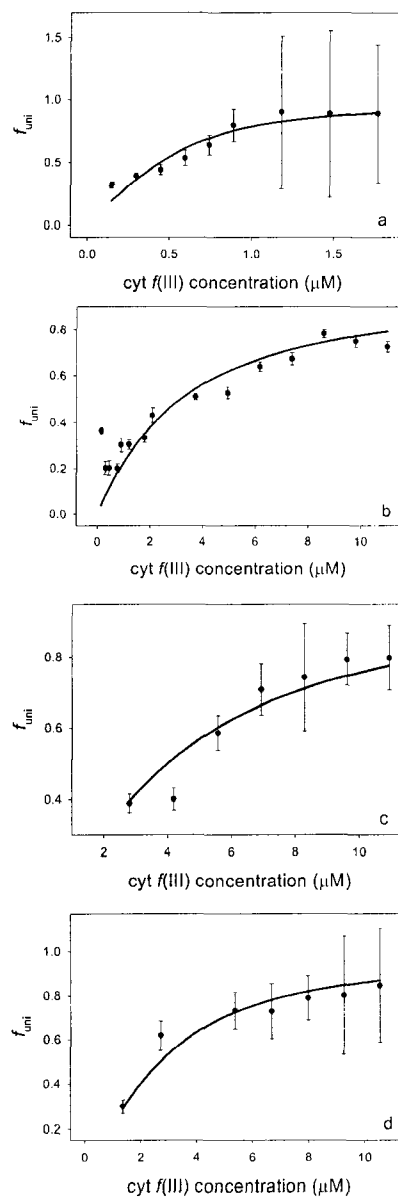
Figure S1. Relative amplitudes for the unimolecular kinetic phase in the oxidative quenching of ^{3}Zncyt c_6 by cytochrome f(III) in sodium phosphate buffer at pH 7.0 at room temperature, and ionic strength of (a) 2.5 mM, (b) 10 mM, (c) 300 mM, and (d) 700 mM. Concentration of Zncyt c_6 is: (a) 1 μM, and (b) through (d) 3 μM. Solid lines are fitting to equation 10.
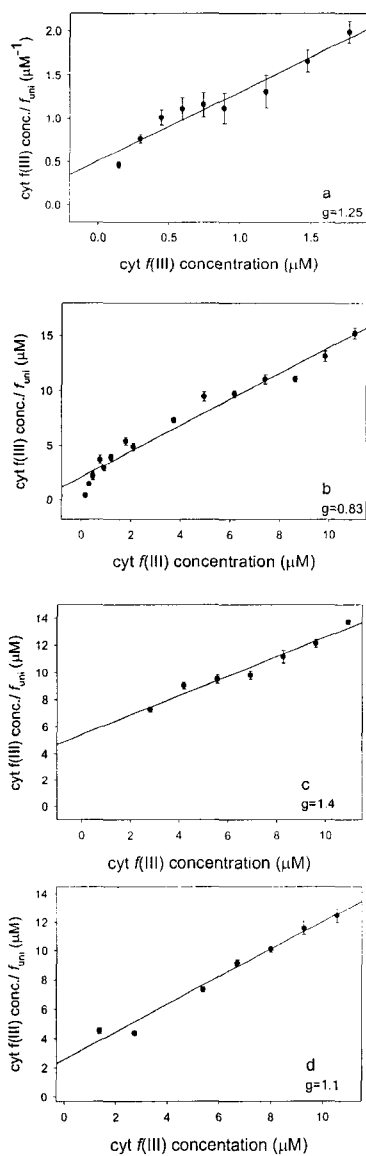
Figure S2. Dependence of the ratio of cytochrome f(III) concentration and relative amplitude for

the unimolecular kinetic phase on the concentration of cytochrome f(III). Solvent is sodium

phosphate buffer at pH 7.0 at room temperature, and ionic strength of (a) 2.5 mM, (b) 10 mM, (c)

300 mM, and (d) 700 mM. Concentration of Zncyt c_6 is: (a) 1 μM, and (b) through (d) 3 μM.

Solid lines are fitting to equation 11.
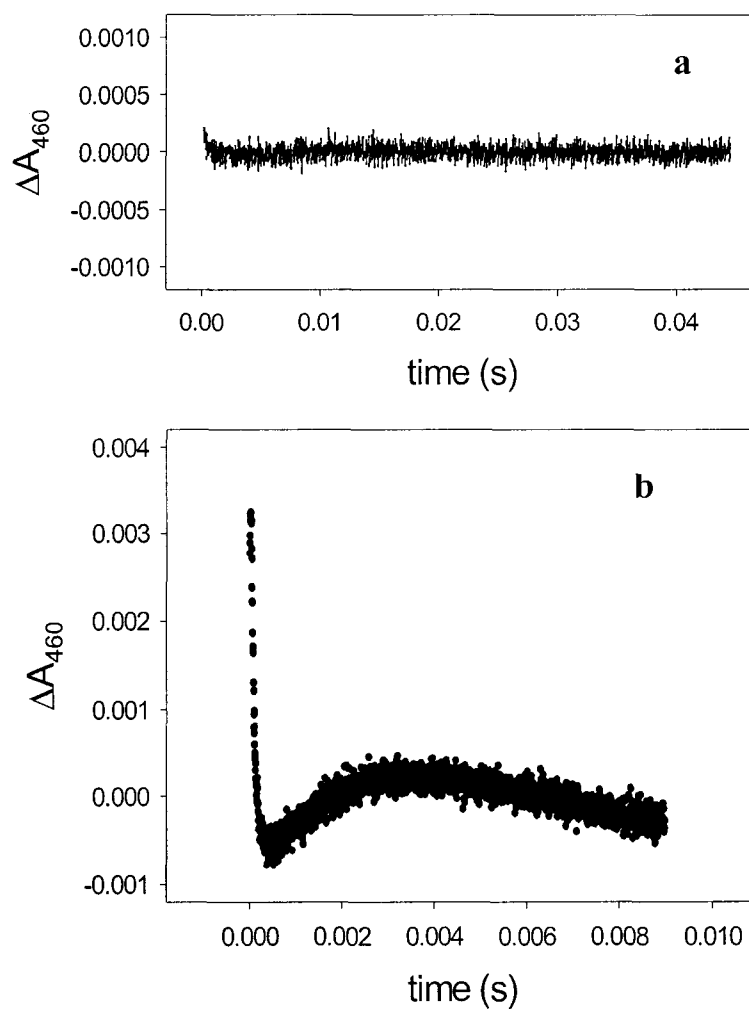
Figure S3. Residuals for the fitting of traces in Figure 9 to the monoexponential function in

eq 12. (a) An attempt at quenching of ^{3}Zncyt c_6 with cross-linked dimer of cytochrome

f(III). (b) Quenching of ^{3}Zncyt c_6 with monomer of cytochrome f(III). The solvent is

sodium phosphate buffer having pH 7.00 and ionic strength of 300 mM at room
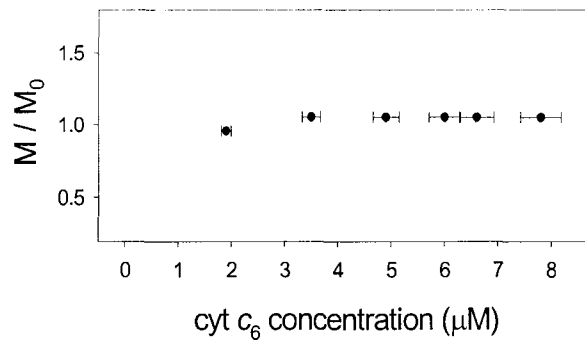
Figure S4. Study by ultracentrifugation of sedimentation equilibrium of cytochrome c_6

dissolved in sodium phosphate buffer at pH 7.0 and ionic strength of 300 mM. Protein

concentration is varied from 2.0 to 8.0 μM. Equality of the effective molecular mass in

solution, M, and the nominal molecular mass, M_0, of this protein at all concentrations rules

out self-association in solution under the experimental conditions.
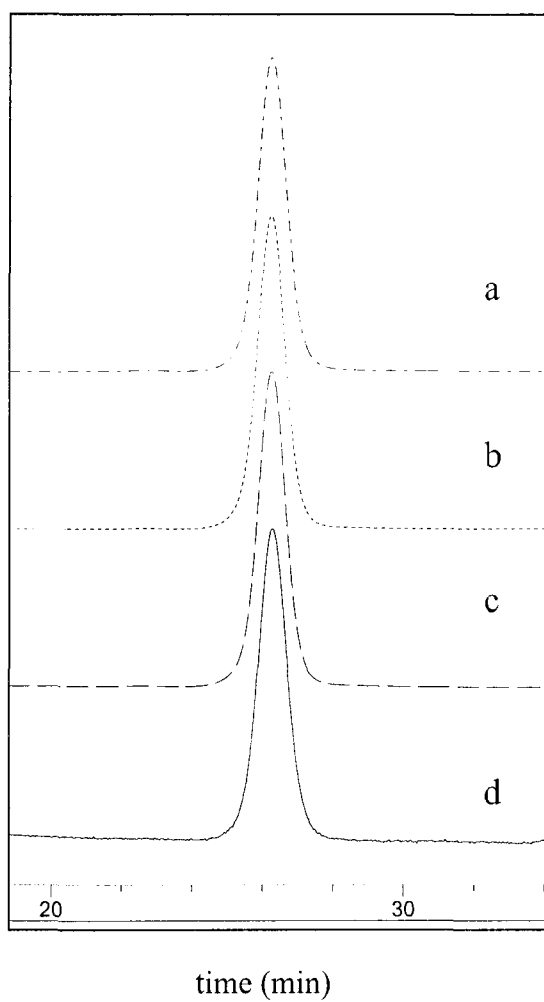
Figure S5. Size-exclusion HPL chromatograms of *C. reinhardtii* cytochrome c_6 obtained

with a 100 mM (concentration) sodium phosphate buffer at pH 7.0 as eluent. Concentration

of the protein is: (a) 50 μM, (b) 10 μM, (c) 5.0 μM, and (d) 1.0 μM. Elution time of ca. 26

min is diagnostic of the monomer.

CHAPTER 3. SIMULTANEOUS TRUE, GATED, AND COUPLED ELECTRON-TRANSFER REACTIONS AND ENERGETICS OF PROTEIN REARRANGEMENT

A paper prepared for journal submission

Tijana Ž. Grove[1], G. Matthias Ullmann[2], and Nenad M. Kostić[1,*]

[1]Department of Chemistry, Iowa State University, Ames, Iowa 50010 and [2]Structural

Biology/Bioinformatics, University of Bayreuth, Universitätsstr. 30, BGI 95447 Bayreuth,

Germany

The Brownian Dynamics calculations were done by Prof. G. Matthias Ullmann. All kinetic

experiments, fittings, and interpretation of results were done by the primary author.

Abstract

We study, by laser flash photolysis, effects of temperature and viscosity on docking and

kinetics of the electron-transfer reaction between cytochrome c_6 and its physiological partner

cytochrome f, both from *Chlamydomonas reinhardtii*. The hydrophobic interaction is

energetically comparable, $\Delta H_a = (4\pm1)$ kJ/mol, and $\Delta S_a = (127\pm4)$ JK^{-1}mol^{-1}, to electrostatic

interaction reported for different protein pairs. The net reaction ^{3}Zncyt c_6 + cyt f(III) $\rightarrow$

Zncyt c_6^+ + cyt f(II) occurs within the persistent complex of the associated proteins

(concentration-independent path) with the rate constant k_{pr} and within the transient complex

of the colliding proteins (concentration-dependent path) with the rate constant k_{tr}. Biphasic

kinetics and detectable kinetic intermediate, Zncyt c_6^+, in the entire temperature interval

studied, from 0.5 to 40.0 °C, show that the two-path mechanism operates throughout. The

independence of the rate constant k_{pr} on viscosity, and analysis of Marcus parameters,

H_{ab}=(0.5 ± 0.1) cm^{-1}, λ=(2.14 ± 0.02) eV, indicates that reaction within persistent complex is

true electron transfer. The Eyring plot for the reaction within transient complex has a cusp

that corresponds to the temperature of ca. 303 K, $\Delta H_{tr}^{\neq}$=(18.4 ± 0.4) kJ/mol, and $\Delta S_{tr}^{\neq}$=(-122

± 10) JK^{-1}mol^{-1} for the temperature below, and $\Delta H_{tr}^{\neq}$=(-52 ± 1) kJ/mol, and $\Delta S_{tr}^{\neq}$=(-350 ± 30)

JK^{-1}mol^{-1}, for the temperature above ca. 303 K. The rate constant k_{tr} is viscosity-dependent

throughout the studied temperature range (283 K-313 K). Protein friction parameters

obtained from two forms of Kramers's equation differ drastically for the reaction below ca.

303 K [σ=(0.3 ± 0.1), δ=(0.85 ± 0.07)], and for the reaction above [σ=(4.0 ± 0.9), δ=(0.40 ±

0.06)]. Intracomplex reaction for the transient complex is coupled electron transfer for

temperatures below ca. 303 K and is analyzed by an equation that combines adiabatic

rearrangement step followed by nonadiabatic electron transfer. The same reaction is gated

electron transfer at the temperatures above ca. 303 K.

Introduction

Long-range inter-protein electron transfer is essential for the controlled flow of the electrons

in biological energy transduction. In physiological processes such as respiration,

photosynthesis, and metabolic redox reactions, mobile redox proteins transport electrons

between membrane-bound protein complexes.[1,2] These biological processes could be

properly understood only if protein interactions and reactions are understood on the

molecular level.[3-6] Despite vigorous current research that utilizes a multidisciplinary

approach, mechanisms of electron-transfer reactions of metalloproteins are only partially

understood. [7]

It is widely accepted that the same pair of redox proteins may form multiple complexes that may undergo essentially the same intracomplex electron-transfer (et) reaction at different rates.[5,6] A number of cases have been observed in which reactant complex is undergoing dynamic fluctuations in configuration, but little is known about energetic contribution of the intracomplex rearrangement to the overall et mechanism.[4,8-10] We go step beyond intuitive notion of facile interconversion between different binding configurations of diprotein complex by determining not only rate constants, but also equilibrium constants and estimates of activation barriers for dynamic rearrangement. Recently, new paradigm in protein-protein interaction and dynamics was designated as the "Dynamic Docking" (DD), in which a large ensemble of bound protein-protein conformations contributes to binding, but only some of them are reactive.[5]

The overall reaction in eq 1 involves protein association, rearrangement (equilibrium constant $K_r = \dfrac{k_r}{k_{-r}}$) of the initial configuration(s) (subscript i) into the reactive one(s) (subscript r), and electron transfer. The rearrangement and

$$A_{ox} + B_{red} \underset{k_{off}}{\overset{k_{on}}{\rightleftharpoons}} [A_{ox} - B_{red}]_i \underset{k_{-r}}{\overset{k_r}{\rightleftharpoons}} [A_{ox} - B_{red}]_r \overset{k_{et}}{\longrightarrow} [A_{red} - B_{ox}] \qquad (1)$$
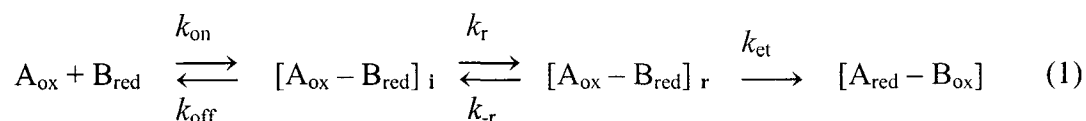
et steps are differently combined in true, gated, and coupled mechanisms for et.[7,11] In *true* et mechanism, the rate-limiting step is electron transfer ($k_{et} < k_r$), and the apparent rate constant is simply k_{et}. Reorganizational energy for the et step, λ, can be determined by fitting of kinetic results to Marcus theory. In *gated* et mechanism the rate-limiting step is the rearrangement ($k_{et} > k_r$); although et is experimentally monitored, the apparent rate constant is k_r. Now, attempts at fitting to Marcus theory are thwarted by the seeming dependence of the observed reorganizational energy λ on the free energy of rearrangement, ΔG_r. In *coupled*

et mechanism et is the slow step ($k_{et} < k_r$). The faster, but thermodynamically unfavorable (K_r < 1) rearrangement affects the apparent rate constant, which is the product $K_r \bullet k_{et}$. Fitting to Marcus theory yields a composite λ that has contributions from both et and rearrangement steps.[7,11] This recent classification in terms of kinetic observables and the λ parameter is useful. Here, we ground this categorization in reaction mechanisms and energetics.

True and gated et reactions between metalloproteins are known, but coupled reactions are still rare and are often conflated with gated reactions. These three mechanisms have been elegantly diagnosed, but in studies with different proteins.[10,12-16] It is therefore unclear whether the diversity in reactivity comes from differences among the proteins or from kinetic factors.

To reach a unified view of protein reactivity, the aforementioned three mechanisms need to be compared for the same protein pair. We found such a case. We report that different mechanisms can occur simultaneously and can be turned on and off by small changes in temperature. We estimate the rate constants k_r and k_{-r}, the equilibrium constant K_r, and the activation barrier $\Delta G_r^{\ddagger}$ for the protein rearrangement required for et.

$$^{3}\text{Zncyt } c_6 + \text{cyt} f(\text{III}) \rightarrow \text{Zncyt } c_6^{+} + \text{cyt} f(\text{II}) \qquad (2)$$
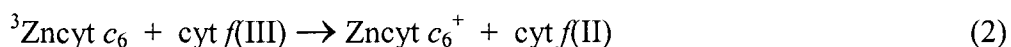
Dynamic mobility and its energetics are governed by protein-protein docking and surface interactions. If the rearrangement step of interest is to become rate limiting and observable, et step must be relatively fast. We achieve this by replacing iron ion in cyt c_6 with zinc and making redox step photoinduced. The "mutation" of the metal in the protein interior does not affect interaction of the Zn substituted protein with reaction partner and allows reaction in eq 2 to be well suited system for studying dynamic rearrangement of the diprotein complex interface, which is indeed necessary for efficient physiological et reaction.[8,17] In addition to this, photoinduced reactions do not require external redox agents in

solution to initiate reaction by reduction or oxidation of one of the proteins. Since temperature and viscosity change will affect both initiation reaction and reaction of interest, the interpretation of results would be ambiguous. Because in photoinduced reactions interprotein et is triggered by photons, variation in solution conditions will affect only reaction of interest. Although et reaction in eq 2 is not strictly biological, photoinduced reaction brings to light conformational motions that are crucial for biological functions. Reconstitution of the heme in cyt c_6 with zinc further eliminates complications arising from the studies of two heme proteins. Because cyt c_6 and cyt f are heme proteins, whose absorption spectra overlap, it is almost impossible to follow spectroscopically the simultaneous oxidation of one heme group and reduction of the other.[18]

We use kinetics of the photoinduced reaction in eq 2 to explore kinetics and energetics of dynamic rearrangement within cyt f/ Zncyt c_6 complex that corresponds to the process k_r shown in eq 1. Investigation of temperature and viscosity dependence of the apparent rate constant for the photoinduced reaction in eq 2 reveals that et reaction between zinc cytochrome c_6 and Fe(III) cytochrome f, occurs in all three regimes. More over, the system can be simply manipulated between regimes. This is the first case, to our knowledge, that same net reaction (oxido-reduction in this case) within one metalloprotein pair occurs simultaneously as true and gated, or true and coupled et. We show that difference between three regimes, true, coupled, and gated, is not semantic but real. Furthermore, these regimes can be distinguished experimentally.

Photoinduced ET Reaction between Zncyt c_6 and Cyt f(III)

The mechanism of photoinduced reaction is presented in Scheme S1. Laser flash produces the triplet state of zinc porphyrin, ^{3}Zncyt c_6, which is strong reducing agent. The high driving force (1.2 V) for the photoinduced reaction, makes et step from the triplet state of Zncyt c_6 to cyt f(III), relatively fast and non-et dynamic processes observable. In the absence of a quencher, natural decay of the triplet state of the porphyrin to its ground state in monoexponential (k_{nd} = 100±10 s^{-1}). In the presence of the cyt f(III) decay of the triplet accelerates and is well described with two exponentials. Zncyt c_6 exist in solution as unassociated (free), and associated with cyt f(III) (bound). ^{3}Zncyt c_6 formed by excitation of bound Zncyt c_6 is oxidatively quenched with the rate constant k_{et}^{pr} in unimolecular reaction within **persistent** complex (right-hand side of Scheme S1). When the porphyrin of free Zncyt c_6 is excited to triplet state it associate with cyt f(III)to form **transient** complex and unimolecular reaction of electron transfer occurs, with rate constant k_{et}^{pr}, (left-hand side of Scheme S1). The rate constant k_{et}^{pr}, for the faster of the two phases, is independent of concentration of cytochrome f(III), but the apparent rate constant k^{tr}, for the slower phase, increases and then levels off at relatively high cytochrome f(III) concentrations. To avoid complications arising from dependence of k^{tr} on concentration of cytochrome f(III) protein concentrations are adjusted so that cytochrome f(III) is in excess over zinc cytochrome c_6. Consequently, maximal value of k^{tr} is achieved. It is important to notice that et within persistent and transient complexes is unimolecular reaction. The intracomplex rate constants for the persistent (k_{et}^{pr}) and transient (k^{tr}) complexes in Scheme S1 differ as much as thirteenfold, k_{et}^{pr}=(1.2 ± 0.1) × 10^4 s^{-1}, and k^{tr}=(9 ± 4) × 10^2 s^{-1} in the 10mM phosphate buffer at pH=7.00 and at room temperature.[10]

Kinetic Effects of Temperature

Classical transition-state theory, from which eqs 3 and 4 are derived, assumes that the probability of the reaction occurring when activation energy is achieved is approximately unity. In that case eq 3 shows enthalpy and entropy of activation that describes transition state for the reaction. et reactions are nonadiabatic and Marcus theory, eqs 5 and 6, is modified form of transition-state theory that takes into account nonadiabacity of et reactions.

$$k = \frac{k_B T}{h} \exp\frac{\Delta S^{\neq}}{R} \exp\frac{-\Delta H^{\neq}}{RT} \tag{3}$$

$$\Delta G^{\neq} = \Delta H^{\neq} - T\Delta S^{\neq} \tag{4}$$

$$k = \frac{4\pi^2 H_{AB}}{h(4\pi\lambda RT)^2} \exp\left[\frac{-(\Delta G^0 - \lambda)^2}{4\lambda RT}\right] \tag{5}$$

$$k = k_0 \exp[-\beta(r - r_0)] \exp\left[\frac{-(\Delta G^0 - \lambda)^2}{4\pi RT}\right] \tag{6}$$

Biphasic kinetics and detectable $Zncytc_6^+$ in the entire interval studied, from 0.5 to 40.0 $^{\circ}$C, show that the two-path mechanism in Scheme S1 operates throughout. We fitted temperature dependence of k^{pr} and k^{tr} to eq 3 to determine enthalpy ($\Delta H^{\neq}$) and entropy ($\Delta S^{\neq}$) of activation, and then obtained free energy of activation ($\Delta G^{\neq}$) with eq 4. Since the interpretation of activation parameters for nonadiabatic et reactions is ambiguous, $\Delta H^{\neq}$, $\Delta S^{\neq}$, and $\Delta G^{\neq}$ are given only for comparison of the processes within persistent and transient complexes. Unexpectedly but consistently, inspection of the top panel of the Figure 1 and comparison of the values for $\Delta H^{\neq}$, $\Delta S^{\neq}$, and $\Delta G^{\neq}$ for the reactions within persistent and transient complexes reveals that there are three different intracomplex recations: that within

the persitent complex and those within the transient complex(es) above and below ca. 30 °C. The "broken" plot in Figure 1a suggests a change of mechanism for the transient complex; this change is reversible by heating and cooling. To our knowledge, such a "broken" Eyring plot has not been reported before for protein et reactions.

Furthermore, analysis of temperature effect on an et reaction in terms of Marcus theory can provide initial diagnosis if reaction is true, or coupled or gated et. Figure 1b and the bottom three rows in Table 1 allow a closer, but still inconclusive, comparison of these three reactions. A λ value between ca. 0.7 and ca. 2.3 eV and $H_{AB} < 80$ cm^{-1} are symptomatic of true et mechanism[7], and we tentatively assign it to the reaction within the persistent complex. A λ value exceeding ca. 2.3 eV is symptomatic of gated et mechanism if accompanied by $H_{AB} > 80$ cm^{-1} and of a coupled et mechanism if accompanied by $H_{AB} < 80$ cm^{-1}. Consistent fittings of k_{IT}^{tr} to eqs 5 and 6 gave the latter combination of results, and we tentatively assign the coupled mechanism to the reaction within the transient complex below ca. 30 °C. Marcus theory does not apply to k_{hT}^{tr} because this rate constant reproducibly decreases as temperature increases. We will discuss this interesting case below.

Edge-to-edge distance between electron donor and electron acceptor is an additional parameter that can be obtained from eq 6 though it is difficult to judge soundness of obtained et distances in the absence of the structure of et active diprotein complex. Brownian dynamics simulation of the association of cyt c_6 and cyt f yielded many different low-energy complexes with interaction energies lower than -8 kT in which the distance between the redox centers varies between 12 and 32 A. The values of distance, r, obtained from fitting of k^{pr} and k_{IT}^{tr} to eq 6 are well within this range.

The study of temperature effects on reaction in eq 2 indicates that we are able to observe three different processes, two of them simultaneously, and that reaction mechanism

within transient complex changes at the temperature of approximately 30°C. Moreover, only k^{pr} and k_{IT}^{tr} correspond to processes that are conceivably et, where k^{pr} is possibly rate constant for the true et and k_{IT}^{tr} rate constant for coupled et, judged from the analysis of the parameters obtained from fitting of these two rate constants to eqs 5 and 6.

However, analysis of the temperature dependence of et reaction rates is not sufficient to say whether monitored reaction is true, coupled, or gated. Studies that include variation of solvent conditions, like viscosity, can provide important information to complement temperature dependence studies. In order to further explore nature of detected processes, we next studied kinetic effects of viscosity.

Kinetic Effects of Viscosity

In previous studies in our laboratory, the solution viscosity was introduced as an experimental variable, to detect structural rearrangement of protein complex. Nonbinding and conformationally noninvasive viscogens increase molecular friction, impede protein motion, and slow down protein rearrangement, without affecting the rate constant for the et step and equilibrium constants.[8,10,12,14-16,19-21] Noneffect of glycerol on K_a is evident in Supporting Material, Fig. S1.

The rate constant k^{pr} does not depend on viscosity, but the apparent rate constant k^{tr} does. Dependence of the rate constants k_{IT}^{tr} and k_{hT}^{tr} on viscosity, shown in Figure 2, was fitted to empirical equations 7 and 8, in which η is solvent viscosity; $\Delta G^{\neq}$ is the free energy of activation for the rearrangement, and σ and δ are parameters related to the protein friction. The eq 7 is modified form of Kramers's theory that recognizes importance of Brownian fluctuation in overcoming energy barrier for a process and assumes existence of more than

two possible configurations. Equation 8 reduces to Kramers's equation when $\delta=1$. Both

equations have been used to detect configurational rearrangement of protein-protein and

peptide-protein complexes.[8,10,12,14-16,19-21] The results of fitting are listed in Table 2.

$$k = \frac{k_B T}{h} \frac{1+\eta}{\sigma+\eta} \exp\left[\frac{-\Delta G_\sigma^{\neq}}{RT}\right] \tag{7}$$

$$k = \frac{k_B T}{h} \eta^{-\delta} \exp\left[\frac{-\Delta G_\delta^{\neq}}{RT}\right] \tag{8}$$

The markedly different values above and below 30 °C in Table 2 confirm that

temperature change effects a mechanism change in the transient complex. Because σ and δ

values depend on the protein surfaces accessible to solvent, and exposed surfaces in turn

depend on buried surfaces, the interface in the transient complex seems to change around 30

°C. Viscosity effects confirmed that the same two proteins react by three different

mechanisms, which will be discussed separately below.

Reaction Within the Persistent Complex

The small H_{AB} and reasonable λ values in Table 1 and viscosity independence of k^{pr}

consistently indicate that the persistent complex undergoes a nonadiabatic, true et reaction.[7]

The negative value - 158 $JK^{-1}mol^{-1}$ in Table 1 suggests that considarable "tightening" of the

complex is involved in its activation for the et step.[14]The persistent complex evidently is

dynamic. We surmise that only some of its configurations are et-active, and that

configurational fluctuation probably is too fast to affect the et step, which then is rate-

limiting. It is tempting to attribute the aforementioned Marcus parameters to the et-active

configurations of the persistent complex, but direct evidence is unobtainable.

Reactions Within the Transient Complex

Since photoinduced reactions have high driving force, it is conceivable that with increase in temperature $-\Delta G^\circ$ becomes larger than λ. The situation where $-\Delta G^\circ > \lambda$ corresponds to Marcus inverted region.[22] For the photoinduced reaction in eq 2 to switch from normal to inverted Marcus region, its driving force (ΔG^0) would have to increase from 1.3 eV, the value for the persistent complex, to at least 2.0 eV, the magnitude of λ. The change of 0.7 eV or more within a temperature interval of only 40 °C is improbable. Interplay between the complex rearrangement and et is much more reasonable cause of the temperature dependence of k^{tr}.

Both $\Delta H^{\neq}$ and $\Delta S^{\neq}$ in Table 1 markedly change as temperature crosses the 30 °C mark. Moreover, these two changes compensate each other and are invisible in the composite $\Delta G^{\neq}$ values. That $\Delta S^{\neq}$ is negative for both branches of the "broken" Eyring plot in Figure 1 suggests that structural "tightening" of the complex, presumably to improve the donor-acceptor coupling, is required for et in all cases.[14] That the $\Delta S^{\neq}$ values are very different for the two branches of the plot confirms that the et mechanisms are different in the two temperature intervals. Next, we will discuss these two intervals separately.

Gated ET Reaction, Above ca. 30°C. The rate constant for the reaction within transient complex that corresponds to the high-temperature branch of Eyring plot is decreasing with the temperature. As we discussed previously, this is impossible for the interprotein et. Therefore, we will discuss k^{tr}_{hT} in terms of non-et processes in eq 1. Indeed, viscosity dependence of k^{tr}_{hT} (Figure 2) is diagnostic of structural rearrangement. The most striking feature of the reaction within transient complex at high temperature is negative value of activation enthalpy (Table 1). Negative $\Delta H^{\neq}$ values are rare, and we think unknown for

metalloprotein reactions. Two general explanations exist.[23,24] In one, the reaction mechanism

may involve an enthalpically favorable and fast preequilibrium step.[23] In eq 1 this would be

the rearrangement, defined by K_r. The "pre-equilibrium" condition would require $k_{et} \ll k_{-r}$.

Because k^{pr} in Scheme S1 represents true et, k^{pr} applies to the et step in any mechanism

involving this particular protein pair. We justifiably substitute k^{pr} for k_{et} in eq 1: $k^{pr} = 1 \times$

$10^4 s^{-1} = k_{et}$. Hence the lower limit $k_{-r} > 1 \times 10^4 s^{-1}$ for this gated mechanism. In another

explanation, negative $\Delta H^{\neq}$ with positive $\Delta G^{\neq}$, as in our case, suggests that the transition state

resembles the products.[24] Indeed, in structural interconversion of very similar protein

configurations the transition state and the final state are alike. We cannot choose between

these two plausible explanations of negative $\Delta H^{\neq}$.

Revealingly, different temperature and viscosity experiments and different theoretical

fittings of the apparent rate constant k^{tr}_{hT} gave the same $\Delta G^{\neq}$ values in Table 1 (above 30 °C)

and Table 2 (at 40 °C). This equality of the $\Delta G^{\neq}$ values corroborates the notion that the

apparent rate constant k^{tr}_{hT} corresponds to a complex rearrangement, which is slower than the

et step and therefore rate-limiting for the overall process in eq 1. We conclude that the

reaction within the transient complex above 30 °C occurs by the gated mechanism.

Coupled ET Reaction, below ca. 30°C. The H_{AB} value consistent with a

nonadiabatic reaction and λ value considerably greater that that expected of true et

mechanism, occuring together, are diagnostic of a coupled mechanism[11], which should not be

confused with the more common gated mechanism. In the coupled mechanism the apparent

rate constant depends on the slowest step, which is et, but also on the rearrangement

preceding et because this rearrangement, although faster than et, is thermodynamically

unfavorable. The question is whether et that is coupled by configurational rearrangement of

diprotein complex could be distinguished from gated et. In previous work we expressed

rational skepticism to whether solution viscosity can be used to distinguish between coupled and gated reactions.[10,25,26] Here we show that careful analysis of viscosity dependence data, in conjunction with temperature dependence studies, is reliable tool for characterizing et mechanisms.

Because the apparent rate constant k_{IT}^{tr} depends on viscosity, the process represented by k_{IT}^{tr} includes contribution from protein motion. This is one symptom of the coupled mechanism. Now we seek evidence for unfavorable equilibrium, the defining feature of this intricate mechanism. We justified above the substitution of k^{pr} for k_{et} in eq 9. Since both rate constants k_{IT}^{tr} and k^{pr} in eq 9 are known from independent experiments, the equilibrium constant is simply obtained with eq 10.

$$k_{IT}^{tr} = K_r \bullet k_{et} = K_r \bullet k^{pr} \tag{9}$$

$$K_r = \frac{k_{IT}^{tr}}{k^{pr}} = \frac{9 \bullet 10^2 \, s^{-1}}{1.2 \bullet 10^4 \, s^{-1}} = (0.08 \pm 0.04) \tag{10}$$

The value $K_r < 1.0$ agrees with coupled mechanism.[11] Conversion with eq 11 gives ΔG_r^0, the result that comes ultimately from rate constants k_{IT}^{tr} and k^{pr} at a given temperature. To verify coupled mechanism, we determined ΔG_r^0 again, differently. We combined Eyring and Marcus theories in the new eq 12 and applied this hybrid theory to apparent rate constant k_{IT}^{tr}, which, as eq 9 shows, is a product of two factors amenable to these two theories.

$$\Delta G_r^0 = -RT \ln K_r \tag{11}$$

$$k_{IT}^{tr} = \exp\frac{\Delta S^0}{R} \exp\frac{-\Delta H^0}{RT} \bullet \frac{4\pi^2 H_{AB}}{h(4\pi\lambda RT)^2} \exp\left[\frac{-(\Delta G^0 - \lambda)^2}{4\lambda RT}\right] \tag{12}$$

We justifiably fixed the parameters λ and H_{AB} to true-et values in Table 1. Then, fitting temperature dependence of k_{IT}^{tr} to eq 12 gave $\Delta H_r^0 = 16 \pm 3$ kJ/mol and $\Delta S_r^0 = 34 \pm 8$ JK^{-1}mol^{-1}. Plugging those values into eq 13 gave ΔG_r^0, the result that comes ultimately from k_{IT}^{tr} at various temperatures. The satisfying agreement of the ΔG_r^0 values obtained in two different ways further corroborates our proposition, at the beginning of this subsection, that the mechanism is coupled et.

The relative smallness of the value for ΔS_r is in agreement with rapid but overall unfavorable protein rearrangement within diprotein complex that would cause only subtle changes in overall structure.[11] If step preceding et is configurational rearrangement of the diprotein complex, than the effects of coupling would be manifested mainly in a large value of λ with relatively accurate distance between redox centers and value of H_{AB}. The positive value of ΔS_r would yield experimentally determined value of H_{AB} larger that the true value and distance would be smaller than the actual et distance.[11] Comparing values of H_{AB}, and r in Table 1 for k^{pr} (true et) and k_{IT}^{tr} we see that this is the case lending additional support to suggestion that unimolecular reaction within transient complex, at temperature lower that app.30°C, is coupled et. Since standard Marcus theory does not recognize dynamic factors such as protein rearrangement, coupled et is better treated with our eq 12, which recognizes an interplay between rearrangement and et steps.

As explained above, $k_{et} = 1 \times 10^4$ s^{-1} for this protein pair. The defining criterion of coupled et mechanism, stated in the Introduction, gives the lower limit $k_r > 1 \times 10^4$ s^{-1} for this diprotein system. Difference between λ values for the coupled and true reactions in Table 1 is approximately 1.0 eV. Because Marcus theory does not fully apply to coupled et reactions, this difference is uncertain. Semiquantitatively, however, this increment of ca. 1.0 eV may be

taken as the additional reorganizational energy, beyond that for true et, required for coupling of the et step with protein rearrangement.

Configurational Heterogeneity and Energetics of the Protein Complex

Electrostatic and hydrophobic forces govern affinity and specificity of metalloprotein association. In a simple case single binding configuration will be reactive configuration as well. The more complex case is where the most stable binding configuration is not reactive configuration, and et kinetics may be influenced by the rates and energetics of intracomplex conformational rearrangement. In the "dynamic docking" model it is assumed that interconversion between binding configurations is allowed. The question is how this facile interconversion affects the rate constant for et event.

Figure 3a shows a remarkable "energy seascape" - two "islands" connected by an "isthmus." Two very broad ensembles of diprotein configurations appear to be "bridged" by relatively few intermediate configurations. The color-coded height of this "land" is proportional to the probability of protein association. The right island, containing the tallest mountain, is much more populated, but very long heme-heme distances likely preclude et. The left island, featuring two lower hills of probability, is less populated, but heme-heme distances are favorable for et.

Both islands would contribute to the thermodynamic association constant K_a, as determined by calorimetry or spectroscopy. Probably only the leftmost region of the left island contributes to the rate constants for rearrangement and et in Scheme S1.[5] By changing temperature and viscosity, we affect the et event little or not at all, but we sample the protein configurations by the energies required for their rearrangement.

The persistent complex in Scheme S1 is probably relatively homogeneous. A significant fraction of these configurations probably are et-active, either because the initial docking was already optimal or because these configurations rearrange easily. These rearrangements are faster than the et step, which therefore becomes rate-limiting. The persistent complex reacts by true et mechanism in the entire interval studied, from 0.5 to 40 $^{\circ}$C.

The transient complex in Scheme S1 is more heterogeneous, because proteins collide in various orientations. Indeed, Figure 3b shows a wide range of heme-heme orientations. More energy-demanding, and therefore slower, rearrangements are needed for arriving in the short-distance region of the left island in Figure 3a. Our experiments below ca. 30 $^{\circ}$C engage a smaller sample, namely configurations that interconvert accross lower activation barriers, in coupled et mechanism. Experiments above ca. 30 $^{\circ}$C engage a larger sample, namely configurations that interconvert across higher barriers, in gated et mechanism.

Because true and gated mechanisms are clearly different but occur simultaneously (above ca. 30 $^{\circ}$C) with the same proteins, we can assess the energetics of gating. We reasonably assume that rate of the et step is governed by activation free energy ($\Delta G^{\neq}$) and not donor-acceptor coupling H_{AB}. Knowing $\Delta G^{0} = 1.3$ eV and $\lambda = 2.0 \pm 0.2$ eV (an average in Table 1), we calculate $\Delta G^{\neq}$ for true et to be $(\Delta G^{0} + \lambda)^{2}/4\lambda = 1.8$ $k_{B}T$. Then $\Delta G^{\neq}$ for the gated mechanism involving cytochrome c_6 and cytochrome f must be > 1.8 $k_{B}T$. Activation free energies for configurational rearrangement of other proteins, and perhaps biomolecules in general, can be estimated similarly. These energies cannot be obtained by fittings to availbale theories, and are useful in analyzing protein dynamics. Our method promises to be a general one.

Conclusion

Two metalloproteins associate in multiple binding configurations that are close in energy, but only few of them are et competent. Depending on the barrier for the interconversion between binding configurations ET reaction will occur as true, coupled or gated. In the light of this study simultaneous occurrence of different regimes of et is not mere peculiarity, but natural consequence of energy landscape with multiple binding configurations that can interconvert. Cyt c_6 and cyt f metalloprotein pair is exceptional in two ways. Association is mainly governed by hydrophobic forces and et kinetics exhibits unprecedented heterogeneity.[10] It is tempting to suggest that these two distinctive characteristics are related and that non-directional hydrophobic interactions are basis for the energy landscape that is suitable for simultaneous occurrence of true and coupled, and true and gated et reaction.

References

(1) Crowley, P. B.; Ubbink, M. *Accounts of Chemical Research* **2003**, *36*, 723-730.

(2) Kurisu, G.; Zhang, H.; Smith, J. L.; Cramer, W. A. *Science (Washington, DC, United States)* **2003**, *302*, 1009-1014.

(3) Gray, H. B.; Winkler, J. R. *Quarterly Reviews of Biophysics* **2003**, *36*, 341-372.

(4) Lasey, R. C.; Liu, L.; Zang, L.; Ogawa, M. Y. *Biochemistry* **2003**, *42*, 3904-3910.

(5) Liang, Z.-X.; Kurnikov, I. V.; Nocek, J. M.; Mauk, A. G.; Beratan, D. N.; Hoffman, B. M. *Journal of the American Chemical Society* **2004**, *126*, 2785-2798.

(6) Yang, H.; Luo, G.; Karnchanaphanurach, P.; Louie, T.-M.; Rech, I.; Cova, S.; Xun, L.; Xie, X. S. *Science (Washington, DC, United States)* **2003**, *302*, 262-266.

(7) Davidson, V. L. *Accounts of Chemical Research* **2000**, *33*, 87-93.

(8) Pletneva, E. V.; Fulton, D. B.; Kohzuma, T.; Kostić, N. M. *Journal of the American Chemical Society* **2000**, *122*, 1034-1046.

(9) Nocek, J. M.; Zhou, J. S.; Forest, S. D.; Priyadarshy, S.; Beratan, D. N.; Onuchic, J. N.; Hoffman, B. M. *Chemical Reviews (Washington, D. C.)* **1996**, *96*, 2459-2489.

(10) Grove, T. Ž.; Kostić, N. M. *Journal of the American Chemical Society* **2003**, *125*, 10598-10607.

(11) Davidson, V. L. *Biochemistry* **2000**, *39*, 4924-4928.

(12) Crnogorac, M. M.; Shen, C.; Young, S.; Hansson, O.; Kostić, N. M. *Biochemistry* **1996**, *35*, 16465-16474.

(13) Hyun, Y.-L.; Zhu, Z.; Davidson, V. L. *Journal of Biological Chemistry* **1999**, *274*, 29081-29086.

(14) Ivkovic-Jensen, M. M.; Kostić, N. M. *Biochemistry* **1997**, *36*, 8135-8144.

(15) Liu, L.; Hong, J.; Ogawa, M. Y. *Journal of the American Chemical Society* **2004**, *126*, 50-51.

(16) Mei, H.; Wang, K.; Peffer, N.; Weatherly, G.; Cohen, D. S.; Miller, M.; Pielak, G.; Durham, B.; Millett, F. *Biochemistry* **1999**, *38*, 6846-6854.

(17) Anni, H.; Vanderkooi, J. M.; Mayne, L. *Biochemistry* **1995**, *34*, 5744-5753.

(18) Hervas, M.; Navarro, J. A.; De la Rosa, M. A. *Accounts of Chemical Research* **2003**, *36*, 798-805.

(19) Ansari, A.; Jones, C. M.; Henry, E. R.; Hofrichter, J.; Eaton, W. A. *Science (Washington, DC, United States)* **1992**, *256*, 1796-1798.

(20) Feng, C.; Kappler, U.; Tollin, G.; Enemark, J. H. *Journal of the American Chemical Society* **2003**, *125*, 14696-14697.

(21) Qin, L.; Kostić, N. M. *Biochemistry* **1994**, *33*, 12592-12599.

(22) Espenson, J. H. *Chemical Kinetics and Reaction Mechanisms*, 1995.

(23) Frank, R.; Greiner, G.; Rau, H. *Physical Chemistry Chemical Physics* **1999**, *1*, 3481-3490.

(24) Yoder, J. C.; Roth, J. P.; Gussenhoven, E. M.; Larsen, A. S.; Mayer, J. M. *Journal of the American Chemical Society* **2003**, *125*, 2629-2640.

(25) Pletneva, E. V.; Crnogorac, M. M.; Kostić, N. M. *Journal of the American Chemical Society* **2002**, *124*, 14342-14354.

(26) Qin, L.; Kostić, N. M. *Biochemistry* **1993**, *32*, 6073-6080.

Table 1. Temperature dependence of the rate constant k^{pr} and k^{tr} (Scheme 1) fitted to Eyring (eqs 3 and 4) and Marcus (eqs 5 and 6) theories.

fitted parameter (unit)	persistent complex, k^{pr}	transient complex, <30°C, k^{tr}_{lT}	transient complex, >30°C, k^{tr}_{hT}	fitting equation
$\Delta H^{\neq}$ (kJ/mol)	2.6 ± 0.1	18.4 ± 0.4	-52 ± 1	3
$\Delta S^{\neq}$ (JK^{-1}mol^{-1})	-158 ± 5	-122 ± 10	-350 ± 30	3
$\Delta G^{\neq}$ (kJ/mol)[a]	49 ± 4	54 ± 6	57 ± 6	4
H_{AB} (cm^{-1})	0.5 ± 0.1	4.9 ± 0.5	n. d.[b]	5
λ (eV)	2.1 ± 0.1	3.1 ± 0.2	n. d.[b]	5
λ (eV)	1.9 ± 0.1	3.0 ± 0.2	n. d.[b]	6

[a] Room temperature.
[b] Fitting to Marcus theory is unjustifiable.

Table 2. Friction parameters and activation parameters for the reaction within transient complex

T (K)	eq 7		eq 8	
	σ	ΔG_{σ} (kJ/mol)	δ	ΔG_{δ} (kJ/mol)
313, (k^{tr}_{hT})	4.0 ± 0.9	59.8 ± 0.2	0.40 ± 0.06	59.0 ± 0.4
293, (k^{tr}_{lT})	0.2 ± 0.1	56.0 ± 0.2	0.82 ± 0.09	55.3 ± 0.2
283, (k^{tr}_{lT})	0.3 ± 0.2	53.2 ± 0.2	0.89 ± 0.05	52.5 ± 0.2
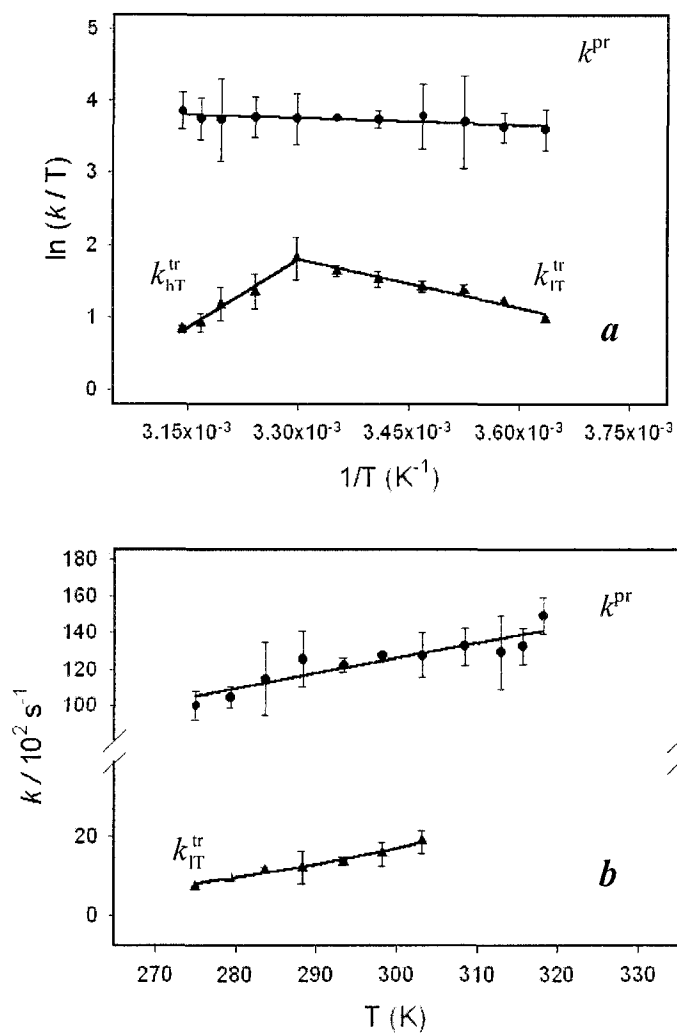
Figure 1. Temperature dependence of the rate constants k^{pr} and the apparent rate constant k^{tr} (Scheme 1) in the sodium phosphate buffer at pH 7.0 and ionic strength of 10 mM. The smallest error bars are invisible. The fitting parameters are given in Table 1. (a) The lines are fittings to eq 3. Data below and above the break at 30 °C were fitted separately, as k^{tr}_{lT} and k^{tr}_{hT}. (b) The fittings to eqs 5 and 6 overlap.
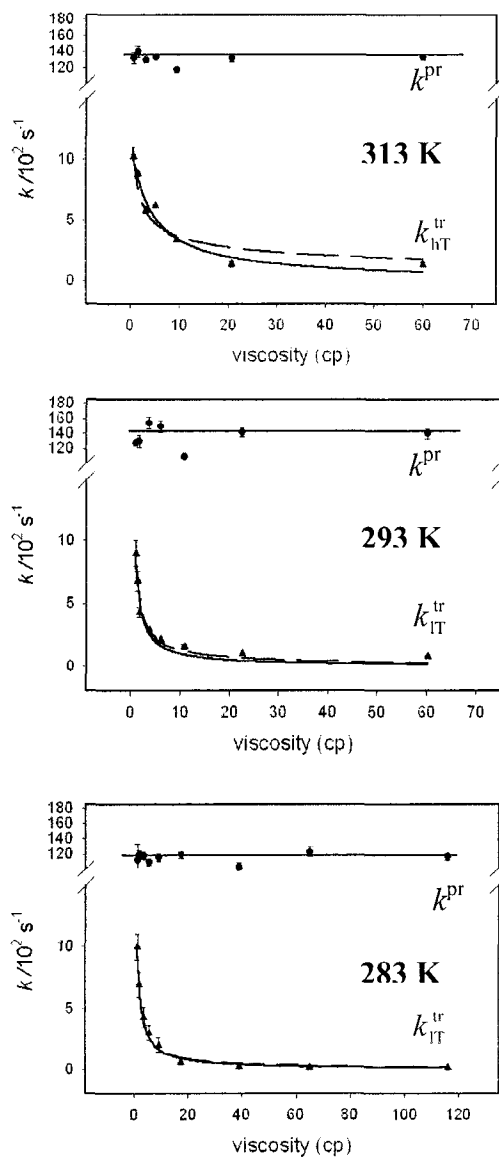
Figure 2. Viscosity independence of the rate constants k^{pr} and viscosity dependence of the apparent rate constants k_{hT}^{tr} and k_{lT}^{tr} in the sodium phosphate buffer at pH 7.0 and ionic strength of 10 mM. . The smallest error bars are invisible. Solid lines are fittings to eq 7; dashed, to eq 8. Fitting parameters are shown in Table 2.
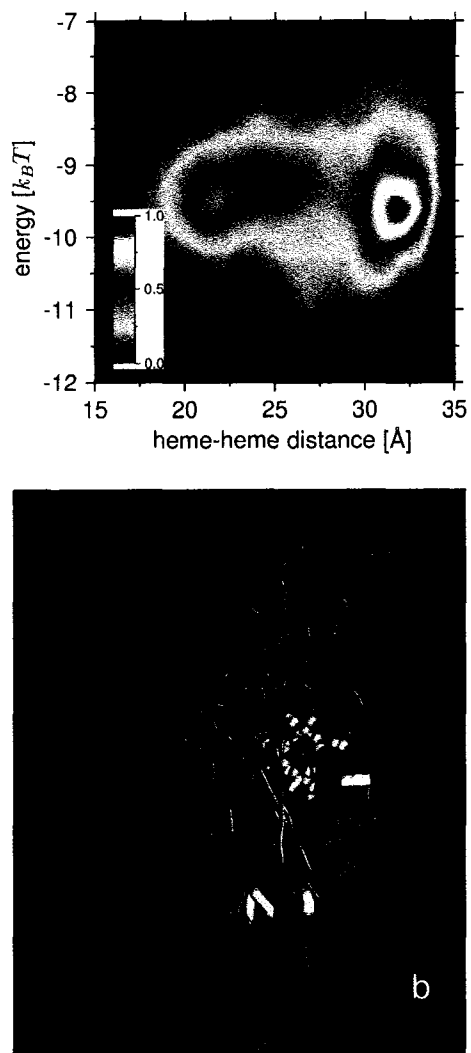
Figure 3. Results of Brownian-dynamics simulation of cytochrome c_6 and cytochrome f at ionic strength of 10 mM. One million trajectories gave about 110,000 diprotein configurations having association energy of -7 k_BT or lower. (a) Probability of association (color-coded) as a function of the protein interaction energy and the shortest heme-heme distance. (b) Cytochrome f and centers of mass of 5000 cytochrome c_6 molecules randomly chosen from 110,000.

Supporting Information

Chemicals and Buffers. Distilled water was demineralized to a resistivity greater

than 17 MΩ cm by a Barnstead Nanopure II apparatus. Chromatographic resins and gels

were purchased from Sigma Chemical Co; hydrogen fluoride, from Matheson Gas Product

Inc; nitrogen and ultrapure argon, from Air Products Co.; all other chemicals, from Fisher

Chemical Co. All buffers were prepared from the solid salts $NaH_2PO_4 \bullet H_2O$ and

$Na_2HPO_4 \bullet 7H_2O$, and had pH of 7.00±0.05 and ionic strength 10 mM.

Proteins. Cytochrome *f* from *C. reinhardtii,* expressed from *E. coli,* was isolated and

purified as described previously.[1] Cytochrome c_6 from *C. reinhardtii* was isolated and

purified by the published method.[2] Iron was removed, and the free-base protein was

reconstituted with zinc(II) ions, by a modification of the standard procedure.[3] Zinc

cytochrome c_6 was always kept in the dark. Concentrations of the two proteins were

determined from their UV-vis spectra, on the basis of known absorptivities: cytochrome *f*(II),

$\Delta\varepsilon_{552}$=26 mM^{-1}cm^{-1}, cytochrome c_6(II), $\Delta\varepsilon_{552}$=20 mM^{-1}cm^{-1}, and zinc cytochrome c_6,

$\Delta\varepsilon_{421}$=(2.3±0.1)*10^5 M^{-1}cm^{-1}.[4] All proteins were stored in liquid nitrogen. Before each series

of experiments, the buffer in protein stock solutions was replaced by the working buffer

using so-called ultrafree-4 centrifugal filter, obtained from Millipore Co.

Laser Flash Photolysis. Experiments were performed with the second harmonic (at

532 nm) of a Q-switched Nd-YAG laser. The instrument was described elsewhere.[4] Argon

was passed first through water and then through the buffer solution. The required volume of

buffer was deaerated in a 10-mm cuvette for at least 30 minutes before proteins were added.

Concentration of cytochrome *f*(III) was 3 μM, and that of zinc cytochrome c_6 was 1 μM .

Decay of the triplet state was monitored at 460 nm, where the transient absorbance has its

maximum. The concentration of the triplet depended on the intensity of the laser pulse and was always much lower than the concentration of cytochrome f(III). Pseudo-first-order excess of cytochrome f(III) was maintained in all experiments. Formation and disappearance of the cation radical were monitored at 675 nm, where the difference between the absorbances of this species and the triplet is greatest. To enhance signal-to-noise ratio, at least 50 shots were collected and averaged each time.

Viscosity. The kinetic effects of viscosity were studied in the 10 mM sodium phosphate buffer at pH 7.0. Glycerol was added incrementally to the solution containing zinc cytochrome c_6 and cytochrome f(III). Because viscosity depends on temperature, these additions were made at each temperature anew, for precise control. The viscosity of the solution was determined from the tables.[5] Solutions were gently deaerated for 10 min after each addition of glycerol.

Temperature. Temperature in the range from 0.5 to 40 °C was kept with a 30-L circulating bath Formaa Scientific CH/P 2067. The actual temperature in the cell was calibrated with an Omega digital thermometar and was known with precision of ± 0.1 °C.

Fittings of the Kinetic Data. The rate constants for the reaction in eq 2 in main text were obtained from the analysis of the changes of absorbance at 460 and 675 nm with time. The former change corresponds to the decay of ^{3}Zncyt c_6 and is a sum of several exponential terms (eq S1). The latter change is caused by both the triplet and the cation radical and is described by eqs S2-S5.[4] Contribution of the triplet to the absorbance change at 675 nm is given by eq S3, in which a_t is the instantaneous absorbance after the laser flash. The contribution of cation radical is fitted with eq S5.

$$\Delta A_{460} = \sum_i a_i \exp(-k_i t) + b \qquad \text{(S1)}$$

$$\Delta A_{675} = \Delta A_{\text{triplet}} + \Delta A_{\text{cation}} \qquad \text{(S2)}$$

$$\Delta A_{\text{triplet}} = a_t \left[\sum_i f_i \exp(-k_i t) \right] \qquad \text{(S3)}$$

$$f_i = a_i / (a_{\text{pr}} + a_{\text{tr}}) \quad i = \text{pr, tr} \qquad \text{(S4)}$$

$$\Delta A_{\text{cation}} = a_c \left[\exp(-k_{\text{fall}} t) - \exp(-k_{\text{rise}} t) \right] \qquad \text{(S5)}$$

Kinetic results were analyzed with the SigmaPlot v.5.0, from SPSS Inc. The error margins for all rate constants obtained from the fitting of the transient-absorbance changes include two standard deviations, i. e, correspond to the confidence limit of 95%. This conservative setting of error margins is a precaution against overinterpretation of small differences.

Brownian Dynamics Simulations. The association of cytochrome f and cytochrome c_6 at ionic strength of 10 mM was simulated using the program Macrodox.[6] The theoretical basis of these simulations in described in detail elsewhere.[6,7] Cytochrome c_6 moved in the electrostatic potential of cytochrome f. The energy was calculated by multiplying the charges of cytochrome c_6 with the electrostatic potential that arises from cytochrome f. The electrostatic potential in these simulations is described by the Poisson-Boltzmann equation.[8] A complex was considered to be formed when its energy was less than -7 k_BT. This cut-off was chosen to get a reasonable number of docked configurations. In Figure 3a, the probability of occurrence of a docked configuration in the most-populated energy-distance bin was set to unity, and populations of other bins were normalized to this value.

Natural Decay of the Triplet State ^{3}Zncytc$_6$. In the absence of a quencher, the decay of the triplet excited state of the porphyrin to its ground state is monoexponential (eq S6). The rate constant for this natural decay, k_{nd}, is 100±10 s^{-1} in the temperature range between 0.5 and 40 °C in the phosphate buffer having pH 7.00 and is independent of protein

concentration in the interval from 1.0 to 10 µM and ionic strength in the interval from 2.5 to 700 mM.

$$\Delta A_{460} = a_{nd} \exp(-k_{nd}t) + b \qquad (S6)$$

Biphasic Oxidative Quenching of the Triplet State $^3Zncytc_6$ by Cytochrome f(III) at all Temperatures. In the presence of cytochrome f(III), decay of the triplet is accelerated over natural decay. The time course of the decay is well described by a biexponential function (eq S7) throughout the whole temperature range, between 0.5 and 40 °C. The rate constant k^{pr} is independent of concentration of the cytochrome f(III), but rate constant k^{tr} levels off at relatively high quencher concentration.[4] We have chosen protein concentrations so that cytochrome f(III) is in an excess over Zn cytochrome c_6.

$$\Delta A_{460} = a_1 \exp(-k^{pr}t) + a_2 \exp(-k^{tr}t) + b \qquad (S7)$$

The rate constants for the appearance and disappearance of the redox intermediate, cation radical, are independent of the cytochrome f(III) concentration. The increase in the absorbance at 675 nm is due to the back reaction (eq S8), and its decrease is due to the forward reaction (eq 2 in the main text).[5]

$$Zncyt\ c_6^+ + cyt\ f(II) \longrightarrow Zn\ cyt\ c_6 + cyt\ f(III) \qquad (S8)$$
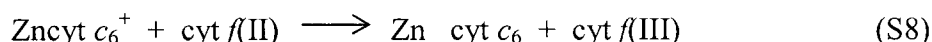
We observed the appearance and disappearance of the cation radical throughout the temperature range studied.

Temperature Dependence of the Rate Constants k^{pr} and k^{tr}. We fitted temperature dependence of k^{pr} and k^{tr} to eq 9 to determine enthalpy ($\Delta H^{\neq}$) and entropy ($\Delta S^{\neq}$) of activation, and then obtained free energy of activation ($\Delta G^{\neq}$) with eq 10 in the main text. Fittings of k^{pr} and k_{IT}^{tr} to Marcus theory (eqs 11 and 12 in main text) gave the heme-heme electronic coupling (H_{AB}) and the reorganizational energy (λ). In the eqs 11 and 12 symbols have their usual meanings: H_{AB} is the electronic coupling between the two redox centers; λ is the

reorganizational energy; h is the Planck's constant; R is the gas constant; k_0 is the nuclear

frequency $(10^{13}s^{-1})$; r_0 is the contact distance (3.0 Å); β is the attenuation of electronic

coupling over distance; and r is donor-acceptor distance. For $\beta=1.0$ and $\beta=1.4$ fitting to

equation S12 yielded the same value of λ within the error bars. The λ shown in Table 1 in the

main text is obtained with $\beta=1.4$.

Kinetic Effects of Viscosity. The reaction in eq 2 in main text was studied at ionic

strength of 10 mM and temperatures 10 ± 1 °C, 20 ± 1 °C, and 40 ± 1 °C. The decay of ^{3}Zncyt c_6

remained biphasic at all temperatures throughout the viscosity range studied. The amplitudes

of both intracomplex reactions were unaffected by viscosity, as Figure S1 shows.

Temperature Dependence of Association between Zinc Cytochrome c_6 and

Cytochrome f(III). Temperature effects on the association constant were studied in the

temperature range from 0.5 to 40 °C. The results in Figure S2 were fitted to equation S11.

$$K_a=\exp(-\Delta G_a/RT) \tag{S9}$$

$$K_a=\exp(\Delta S_a/R)\exp(-\Delta H_a/RT) \tag{S10}$$

$$f^{pr}=(1/2[Zncyt c_6]_0)*\{[Zncyt c_6]_0 + [cyt f(III)]_0 +(\exp(\Delta S_a/R)\exp(-\Delta H_a/RT))^{-1} -$$

$$(([Zncyt c_6]_0+ [cyt f(III)]_0 + (\exp(\Delta S_a/R)\exp(-\Delta H_a/RT))^{-1})^2 - 4[Zncyt c_6]_0[cyt f(III)]_0)^{0.5}\} \tag{S11}$$

Values for enthalpy and entropy of association obtained from the fitting are $\Delta H_a=(4\pm1)$

kJ/mol, and $\Delta S_a=(127\pm4)$ JK^{-1}mol^{-1}. Free energy of association calculated from these two

parameters is $\Delta G_a= - 33$ kJ/mol. From the kinetic experiments, using relative amplitudes, we

calculated the equilibrium constant[4], $K_a=(6\pm2)$ 10^5 M^{-1}, and from the eq S13 $\Delta G_a= -33$

kJ/mol. These values of ΔG_a are obtained from the two different sets of experiments and are

in full agreement.

References

(1) Soriano, G. M.; Ponamarev, M. V.; Piskorowski, R. A.; Cramer, W. A. *Biochemistry* **1998**, *37*, 15120-15128.

(2) Kerfeld, C. A.; Anwar, H. P.; Interrante, R.; Merchant, S.; Yeates, T. O. *Journal of Molecular Biology* **1995**, *250*, 627-647.

(3) Ye, S.; Shen, C.; Cotton, T. M.; Kostić, N. M. *Journal of Inorganic Biochemistry* **1997**, *65*, 219-226.

(4) Grove, T. Ž.; Kostić, N. M. *Journal of the American Chemical Society* **2003**, *125*, 10598-10607.

(5) Pletneva, E. V.; Fulton, D. B.; Kohzuma, T.; Kostić, N. M. *Journal of the American Chemical Society* **2000**, *122*, 1034-1046.

(6) Northrup, S. H.; Thomasson, K. A.; Miller, C. M.; Barker, P. D.; Eltis, L. D.; Guillemette, J. G.; Mauk, A. G.; Inglis, S. C. *Biochemistry* **1993**, *32*, 6613-6623.

(7) Madura, J. D.; Davis, M. E.; Gilson, M. K.; Wade, R. C.; Luty, B. A.; McCammon, J. A. *Reviews in Computational Chemistry* **1994**, *5*, 229-267.

(8) Ullmann, G. M.; Knapp, E.-W.; Kostić, N. M. *Journal of the American Chemical Society* **1997**, *119*, 42-52.

$$\text{Zncyt}c_6 + \text{cyt}f(\text{III}) \xrightleftharpoons[k_{\text{off}}]{k_{\text{on}}} \text{Zncyt}c_6 \,/\, \text{cyt}f(\text{III})$$

$hv \quad\Big\updownarrow\quad k_{\text{nd}}$

$$^3\text{Zncyt}c_6 + \text{cyt}f(\text{III})$$

$k_{\text{on}} \quad\Big\updownarrow\quad k_{\text{off}}$

$$^3\text{Zncyt}c_6 \,/\, \text{cyt}f(\text{III})_{\text{ i}}$$

$k_{\text{r}} \quad\Big\updownarrow\quad k_{\text{-r}}$

$hv \quad\Big\updownarrow\quad k_{\text{nd}}$

$$^3\text{Zncyt}c_6 \,/\, \text{cyt}f(\text{III})_{\text{ r}} \qquad\qquad ^3\text{Zncyt}c_6 \,/\, \text{cyt}f(\text{III})$$

transient $\qquad\qquad$ **persistent**

$k_{\text{et}}^{\text{tr}} \qquad\qquad k_{\text{et}}^{\text{pr}}$

$$\text{Zncyt}c_6{}^+ \,/\, \text{cyt}f(\text{II})$$

$\Big\downarrow$ fast

$$\text{Zncyt}c_6 \,/\, \text{cyt}f(\text{III})$$
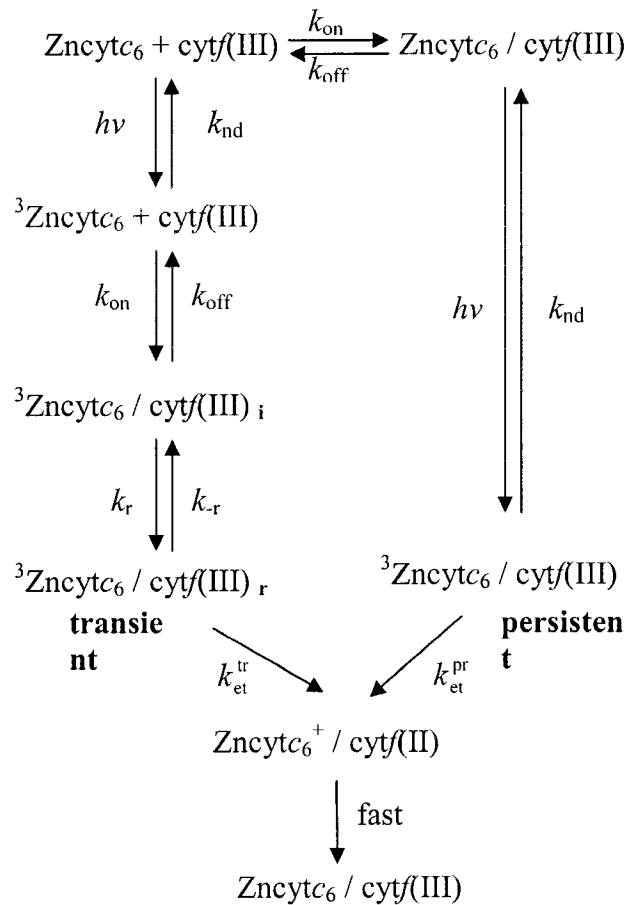
Scheme S1. Kinetic mechanism
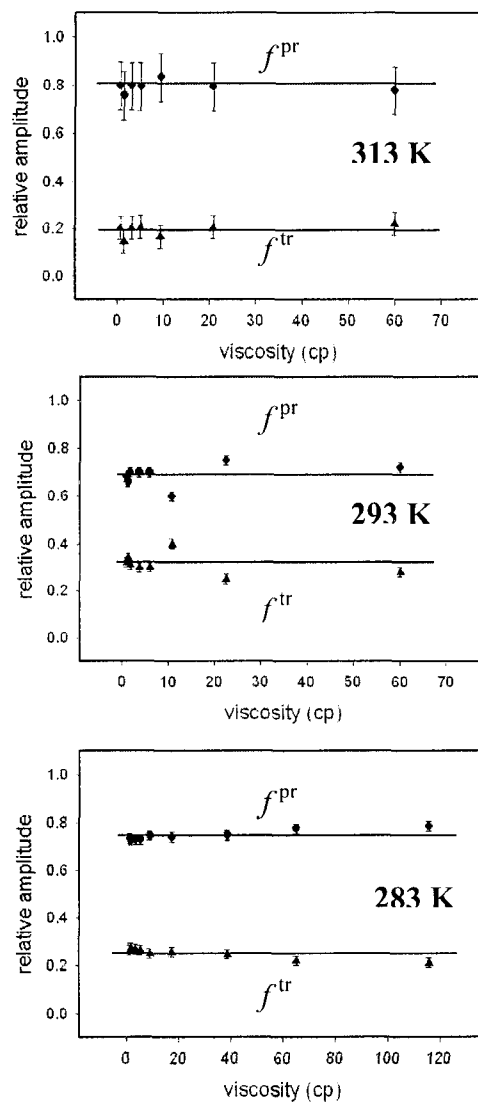
Figure S2. Independence of solution viscosity of the relative amplitudes f^{pr} and f^{tr}, respectively, of the electron-transfer reaction occurring within persistent (•) and transient (▲) protein complex in Scheme 1 at different temperatures. Viscosity of the sodium phosphate buffer solution at pH 7.0, and ionic strength 10 mM was adjusted with glycerol.
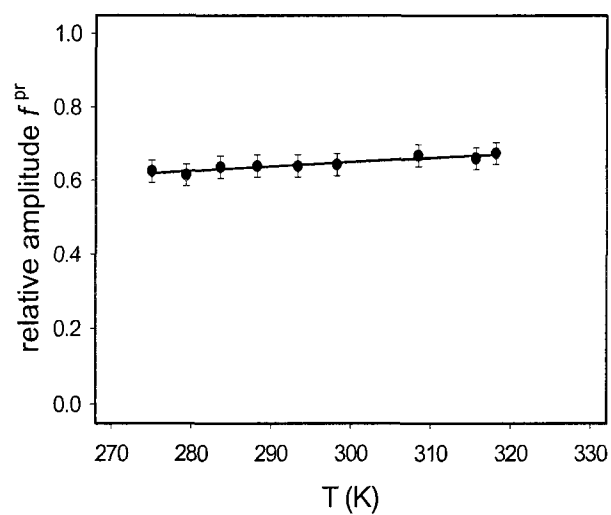
Figure S3. Temperature dependence of the relative amplitude f^{pr} for the reaction between ^{3}Zncytc_6 and cyt$f$(III), in sodium phosphate buffer at pH 7.0 and ionic strength 10 mM. The solid line is fitting to eq S11.

CHAPTER 4. COMPARISON OF PLASTOCYANIN AND CYTOCHROME C_6 IN THEIR REACTION WITH CYTOCHROME F

Introduction

In the processes of biological energy transduction, soluble redox proteins facilitate electron transport between membrane-bound protein complexes.[1-4] In oxygen-evolving photosynthetic organisms, electrons flow from water to ferrodoxin, an iron-sulfur protein that is the starting point for the distribution of electrons for metabolic reactions outside the thylacoide. The electrons are driven uphill from the redox potential of the water/dioxygen couple to the redox potential of the hydrogen electrode. Each electron from water needs two photons to reach the redox level of the hydrogen electrode. Water lysis is carried out by photosystem II (PSII), whereas ferredoxin reduction is performed by photosystem I (PSI). A third membrane-bound complex, that functions between PSII and PSI, is the cytochrome b_6f (cyt b_6f) complex. The three complexes are connected by mobile redox carriers (Figure 1). The transfer of electrons from PSII to cyt b_6f is mediated by hydrophobic quinones, which move in the membrane, while the electron transfer from cyt b_6f to PSI inside the thylacoide vesicle is carried out by soluble metalloproteins, cytochrome c_6 (cyt c_6) or plastocyanin (pc) which are the subject of this study.[1]

Previously, it was widely believed that plants produce only pc, whereas eucaryotic algae and cyanobacteria synthesize either pc or cyt c_6, depending on copper availability.[2,3,5,6] Recently, modified cyt c_6 was discovered in several plants, but the function of this protein is still puzzling.[1,2,7] The structural and functional analysis of plant cyt c_6 revealed that this protein is not an effective donor to its own PSI.[8] The comparative kinetic analysis of redox

reactions of *pc* and cyt c_6 with their physiological partners is thus very interesting not only from mechanistic point of view, but from evolutionary point of view as well.[1,9]

Although they belong to different classes of proteins, *pc* and cyt c_6 perform equivalent reactions with common partners. Extensive investigative effort has been aimed toward establishing the structure-function relationship that allows these two proteins to have identical function despite their different structure.[1,10-14] The *C. reinhardtii* system is of particular interest because it is the first photosynthetic organism examined capable of using both *pc* and cyt c_6 to transfer electrons to $P700^+$ of PSI at a high rate that is the same for both proteins.[1] Furthermore, the high resolution crystal structures of cyt *f* (lumenal part of cyt b_6f complex), *pc* and cyt c_6 from *C. reinhardtii* have been determined.[6,11,15] However, all the kinetic analysis of cyt *f* oxidation so far has been made only with *pc*. The spectrophotometric study of the electron-transfer (et) reaction between cyt *f* and cyt c_6 by following the redox changes in any of two *c*-type cytochromes is not possible experimentally because of the overlapping chromophores.[1,9]

In our laboratory, we were able to overcome the problem of overlapping chromophores by substituting the redox active Fe(II) in the heme of cyt c_6 with redox inactive Zn(II) ions.[9] It has been shown that this substitution does not significantly perturb the structure of *c*-type cytochromes or their interaction with reaction partners.[16,17] The lowest-lying triplet state of Zncyt c_6 is an excellent reducing agent and is easily created with a laser flash. Additionally, the photoinduced reactions are convenient because external reducing agents are not needed so the interpretation of the kinetic data is unambiguous.[18-20] By following the disappearance of the triplet state of Zncyt c_6 we were able to study et reaction between cyt *f* and cyt c_6. To our knowledge, this is the first time that the et reaction between cyt *f* and cyt c_6 was studied.[9]

The purpose of this work is to summarize the current knowledge on et reactions between cyt f with its biological partners pc and cyt c_6. In this chapter we focus on comparison of cyt c_6 and cyt f kinetic results with available literature data for pc and cyt f reaction.

Since some recent data suggested that the mechanisms of et reaction for cyt f with pc and with cyt c_6 might differ among diverse organisms, we will mostly concentrate on the proteins from *C.reinhardtii*.[13]

Reaction Partners

Cytochrome *f*. Cyt f is the lumen-exposed redox center in the membrane-bound cyt b_6f complex. Its function is analogous to that of the mitochondrial/bacterial cytochrome c_1 of the cyt bc_1 complex.[1] In photosynthetic cells, cyt f is attached to the thylacoid membrane. The soluble form, used for kinetic and structural studies, lacks the last 35 residues that include membrane-anchoring α-helix. The modified protein is redox active in vivo and has optical properties very similar to the "wild-type" protein. It has a redox potential value of +365 mV at neutral pH and molecular mass of ca. 30 kDa. The crystal structure of the truncated form of cyt f from *C. reinhardtii* has been determined with a resolution of 2Å.[11]

Cyt f is made of two distinctive domains with the heme group located near the interface of the domains (Figure 2A). The heme is covalently bound to the protein by thioester bonds through the Cys-X-Y-Cys-His sequence characteristic of c-type cytochromes. The axial ligands are a histidine group and surprisingly, the α-amino group of the N-terminal residue Tyr1. The heme is almost completely buried in a hydrophobic pocket. The two

propionic acid side chains and one of the vinyl groups are the only portions of the heme that are solvent exposed.[11]

Besides the atypical heme axial ligation, the main structural characteristics of cyt f are the cluster of lysine residues shown to be the docking site of pc, and the chain of seven water molecules that extends between the heme pocket and the lysine cluster. Dimerization of cytochrome f in the crystal has recently been considered.[11] Seven possible contacts between the protein molecules were identified and a model for the dimer was proposed. However, because certain angles, calculated on the basis of this model, disagreed with the corresponding angles estimated from the EPR spectra of oriented membranes, the crystallographers concluded that protein-protein orientation in the crystal differs from the orientation in the complex of cyt $b_6 f$, which is believed to be dimeric under physiological conditions.[11] In our previous study[9] we were able to detect the dimerization of cytochrome f from $C.$ $reinhardtii$ in aqueous solution. Covalent cross-linking of cyt f followed by size-exclusion chromatography gave one distinct fraction, whose molecular mass is approximately double that of the protein (monomer). Since ionic strength of this solution is very high (700 mM), so that all electrostatic interactions are cancelled, we concluded that the protein dimer is held together by hydrophobic forces.[9] We can only speculate about the implications in $vivo$ of this process, which we documented in $vitro$. The membrane-bound cyt $b_6 f$ was purified and crystallized as a dimer, but resolution of the structure was low, so it is unclear which cyt $b_6 f$ constituents form the dimer interface. Within thylacoid lumen, cyt f is confined to an intermembrane space only 40-90 Å wide, anchored to the membrane, and associated with Rieske protein.[5] In solution, however, cyt f can diffuse freely. We detected its dimerization at ionic strengths of both 300 and 700 mM, conditions relevant to the ionic strength 300 mM in $vivo$.[21] An interesting feature of this apparent dimerization is the loss of

redox reactivity towards Zncyt c_6. Because the cyt f dimer is formed owing to hydrophobic interactions, it is likely that protein molecules cover each other's nonpolar surfaces and the heme edge is no longer accessible to zinc cyt c_6.[9] To our knowledge this is the first case that kinetics of interprotein electron-transfer reaction is modulated by protein self-association.

Plastocyanin. The pc is a type I copper protein with a redox potential of ca. +370 mV at pH of 7.0. The copper atom is located in a pocket formed by conserved hydrophobic residues. The copper is coordinated by two nitrogen atoms of the imidazole rings of two histidines and two sulfur atoms from one methionine and one cysteine. Comparison of all known crystal and solution structures of different pc indicates that the proteins derived from different species have an almost identical overall fold (Figure 2B). The eight β-sheets form a β-sandwich with the copper atom in the "northern end" of the molecule. The region around the solvent-exposed coordinating histidine is known as the "north side" or "hydrophobic patch" and is implicated in the interaction with PSI. Another potential binding site is a "negative patch" located around the solvent exposed, conserved Tyr83. This site is implicated in interaction with cyt f by virtue of attractive electrostatic interaction.[1,2]

Cytochrome c_6. Cyt c_6 from *C. reinhardtii* is a class I c-type cytochrome that has a redox potential of ca. +350 mV at pH of 7.0. The main structural characteristics of cyt c_6 are a short, two-strand anti-parallel β-sheet in the vicinity of the methionine axial ligand, and a nonpolar area around the heme (Figure 2C).[6] The heme group is covalently bound to the protein chain through two cysteines and the axial ligands are one histidine and one methionine. The heme is largely buried in the protein interior; only the propionate oxygens and the edge of the heme are exposed to solvent. The area around the heme is nonpolar except for two Lys residues and one Asp. Comparative study of surface potential maps for six different cyt c_6 (structurally characterized) revealed a similar charge distribution. In all

cases the surface surrounding the heme groups is distinctively hydrophobic, while most of the negative charges are located on the opposite side from the heme. The surface area surrounding the exposed heme crevice is generally considered to be the site for molecular recognition during electron-transfer which, in the case of cyt c_6, would be hydrophobic.[22]

Structural Comparison of Cytochrome c_6 and Plastocyanin

Despite the great difference in the primary and secondary structure of cyt c_6 and pc there are a number of common features (Figure 1). As expected, the two proteins have comparable physicochemical properties: the molecular mass, electrostatic potential, and isoelectric point.[6,11] Furthermore, they have comparable surface characteristics.[1] Numerous structural studies, mainly molecular dynamics and NMR, were done with the goal of establishing the structure-function relationships that allow cyt c_6 and pc to play the same role.[4,10,13,23-26]

In order to compare cyt c_6 with pc, Ullmann et al.[24] developed a new theoretical model termed FAME. In this approach, cyt c_6 and pc were aligned in a way that maximizes similarities in their electrostatic potential. This study resulted in recognition of the acidic patch in cyt c_6 that consists of five negatively charged residues. By analogy, the acidic patch of pc could be recognition site for cyt f. Moreover, it was implied that the aromatic residue Trp63 in cyt c_6 has a similar role to the Tyr83 in pc.[24]

In 1997, Ullmann et al.[23] performed a theoretical study of association between pc and cyt f. Molecular dynamics simulations, in addition to Monte Carlo method, yielded six possible configurations of the diprotein complex. But only in two of these six complexes was the iron-copper distance less than 30Å. Applying the Pathways method and thermodynamics

calculations to the six configurations with the lowest energy, the authors discovered that the configuration with the highest binding affinity is not the one that provides the best electronic coupling. Implication of this finding is that the initial docking complex with the highest binding affinity needs to rearrange into the complex that is electron-transfer active, the one with the best electronic coupling between the redox sites. This binding picture offered a plausible explanation for an interesting finding that covalently bound diprotein complex of cyt f and pc is unreactive. Cross-links without any tethers make the covalent complex rigid and preclude the rearrangement from the most stable configuration to the most reactive one.[23,27,28]

The Brownian dynamics simulation of the interaction of *C. reinhardtii* cyt f with cyt c_6 and pc concluded that complexes formed between cyt f and cyt c_6 closely resemble those formed between cyt f and pc.[10] In each case, electrostatic attraction between negatively charged residues in cyt c_6 and pc and positively charged residues in cyt f holds the proteins in the proper orientation for electron-transfer. Residues involved in the complex interface are hydrophobic in both cases. Although the most interesting result of this particular study is the similarity between the cyt f/cyt c_6 and cyt f/pc complexes, the method used here has serious pitfalls. While hydrophobic interaction is invoked in complex formation, it is not explicitly included in the calculation. Moreover, the diprotein complexes were not subjected to energy minimization. In order to obtain structures of active electron-transfer complexes in Brownian dynamics simulations, it is necessary to include both hydrophobic interactions and energy minimization.[10]

A combination of NMR data and molecular dynamics allowed a closer look into the structure of the transient complex between pc from spinach and cyt f from turnip.[25] It was determined that both the hydrophobic and acidic patch of pc make contact with the cyt f

surface. A single structure, with the short electron-transfer distance between the heme group of cyt f and copper atom of pc, was obtained under a variety of experimental conditions. The NMR chemical-shift mapping confirmed that both acidic and hydrophobic patches of pc are involved in complex formation with cyt f. In the diprotein complex, pc has a single, well-defined orientation with the tightest contact at the hydrophobic patch. The study suggested that the hydrophobic interaction is responsible for the tight fit between proteins, while electrostatic attraction between the acidic patch of pc and the basic patch of cyt f increases affinity of these proteins for each other.[4,26,29,30]
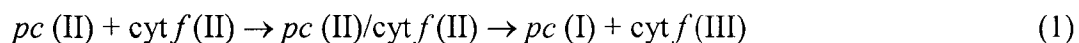
A very recent NMR study characterized the interaction of cyt f from *P. laminosum* and two cyanobacterial cyt c_6 (*Anabena* and *S. elongatus*). *P. laminosum* cyt f utilizes electrostatic attraction for initial docking with *Anabena* cyt c_6, but the interaction site is mainly composed of hydrophobic residues that are involved in complex formation.[4,13] NMR titration of *P. laminosum* cyt f into *S. elongatus* cyt c_6 provided no evidence for specific complex formation but rather very dynamic, nonspecific interaction between these proteins. One of the important conclusions of this very first study on association between cyt c_6 and cyt f is that apparently, the mechanism of electron-transfer reaction for cyt c_6 and pc with their partners will be different for the proteins from the different organisms. Moreover, while in the pc/cyt f complex pc and cyt f have a single, well-defined orientation, the cyt c_6 and cyt f complex is less defined and more dynamic.[13]

Structural studies aimed at comparison of surface properties of cyt c_6 and pc and their implications to the interaction with cyt f, emphasize the similarity of the complex interface in cyt f/cyt c_6 and cyt f/pc complexes.[4,10,13,24] Whether the dynamics and mechanism of electron-transfer reaction will be similar as well requires kinetic study.

The Mechanism of Electron-transfer Reaction

Reaction of PSI with Plastocyanin and Cytochrome c_6. The reaction mechanism and factors influencing reduction of PSI with pc and cyt c_6 have been extensively studied.[1,12,14,31] A number of recent studies have demonstrated that pc and cyt c_6 react with PSI in different ways depending on the organism.[1] The PSI reduction follows monophasic kinetics in most cyanobacteria but a biphasic mechanism in eukariotic organisms and some cyanobacteria.[1] *C. reinhardtii* is the first photosynthetic organism examined capable of using both pc and cyt c_6 to transfer electrons to $P700^+$ of PSI at a high rate that is the same for both proteins.[1] The biphasic kinetics of electron transfer from both pc and cyt c_6 to $P700^+$ in *C. reinhardtii* correspond to a fast first-order reaction within a preformed complex and a bimolecular reaction resulting in second order kinetics. The rate constant for the unimolecular reaction is the same for pc and $P700^+$ and cyt c_6 and $P700^+$. This suggests that cyt c_6 and pc have the same orientation in the binding pocket of PSI with respect to electrostatic and hydrophobic interaction.[14] Mutation and ionic strength studies strongly suggested that electrostatic interactions between the positively charged PsaF subunit of PSI and the negatively charged donor proteins are important for efficient electron transfer. However, at high ionic strength the electron transfer to PSI is inhibited more from pc than from cyt c_6.[1,14]

Reaction between Cytochrome f and Plastocyanin. Because the heme and blue copper chromophores give distinct absorption spectra, reaction of these two proteins can be easily followed. Thus, much research has been done during the past decade on reaction between pc and cyt f.[1,15] The observed rate constant linearly depends on concentration of proteins. The intracomplex rate constant (eq 1) is 2800 s^{-1} in

$$pc \text{ (II)} + \text{cyt} f \text{(II)} \rightarrow pc \text{ (II)}/\text{cyt} f \text{(II)} \rightarrow pc \text{ (I)} + \text{cyt} f \text{(III)} \tag{1}$$

the electrostatic complex but less than 0.1 s^{-1} in the covalent complex obtained by

noninvasive cross-linking.[3,5,21,27,28] This contrast was interpreted in terms of the modulation

of electron transfer in the electrostatic complex by structural rearrangement of pc from a

docking site to the reactive site.[23]

Kinetics and structural studies of the reaction between pc and cyt f indicated that

electrostatic attraction governs the association between these two proteins. The rate constant

for the et reaction between these two proteins decreases monotonically as ionic strength

increases, clear evidence for electrostatic attraction between cyt f and pc.[5,27] In order to

explore protein association, multiple mutants within the basic patch of cyt f were made.[5] In

vitro and in vivo reactions of the wild type and mutant proteins gave somewhat contradictory

results.

The study reported by Soriano et al.[3,5,21] showed that oxidation of cyt f in vitro is rate

limited by the long-range electrostatic attraction between positively and negatively charged

patches on the surface of cyt f and pc, respectively. The positively charged residues that were

subject to mutagenesis were Lys188 and Lys189 in the small domain and Lys58, Lys65, and

Lys66 in the large domain of cyt f. Neutralization of Lys188 and Lys189 caused a decrease in

the ionic strength dependence. Triple mutant Lys58-Lys65-Lys66 had a rate constant of cyt f

oxidation by pc at least 10-fold smaller than wild type, and complete loss of ionic strength

dependence. In the context of in vivo studies[3], in contrast, there was no observable effect of

positive charge elimination on cyt f oxidation by pc. The discrepancy between results

obtained in vitro and in vivo remains unresolved although several feasible explanations have

been offered.[1,5]

Reaction between Cytochrome *f* and Cytochrome c_6. Cyt c_6 and cyt *f* are both *c*-type cytochromes and their absorption spectra overlap. This precludes monitoring the change in oxidation states spectrophotometrically.[1,9] We were able to surmount this difficulty by replacing the heme iron in cyt c_6 with zinc (II) ions. Zncyt c_6 offers many advantages over the native species. It is easily excited by the laser pulse and converted to the triplet state. This long-lived state is a good reducing agent. Another advantage of ^{3}Zncyt c_6 is that external redox reagents are not needed to initiate the reaction between Zncyt c_6 and cyt *f*.[19,20] Although this photo-induced reaction is not strictly biological, it allowed the close look into the dynamics and mechanism of electron exchange between cyt c_6 and cyt *f*. Two studies, described here, and presented in full in the earlier chapters of the thesis, may be the first of that kind.[1,9]

The oxidative quenching of the triplet state of zinc cyt c_6 by cyt *f*(III), reaction (2), was analyzed in terms of protein docking and electron transfer.

$$^3\text{Zncyt } c_6 + \text{cyt} f\text{(III)} \rightarrow \text{Zncyt } c_6^+ + \text{cyt} f\text{(II)} \qquad (2)$$
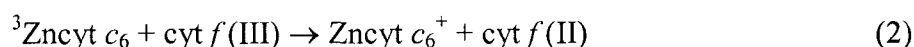
The overall reaction is biphasic. The faster phase corresponds to the concentration-independent, unimolecular reaction within the so-called persistent complex. The slower phase is concentration dependent and corresponds to the bimolecular reaction within the so-called transient complex. The rate constants for both intracomplex reactions, within persistent or transient complex, are ionic strength independent. The association constant K_a for zinc cyt c_6 and cyt *f*(III), obtained from the amplitudes of the two kinetic phases, remains constant in the range from 700 mM to 10 mM, and then rises slightly as ionic strength is lowered to 2.5 mM.[9] Evidently, docking of cyt c_6 and cyt *f* from *C. reinhardtii* is due to strong hydrophobic interaction slightly augmented by weak electrostatic attraction. This hydrophobic interaction is energetically comparable, ΔH_a=(4±1) kJ/mol, and ΔS_a=(127±4)

J/Kmol, to the electrostatic interaction reported for different protein pairs.[32] In contrast to the

interaction of cyt f and pc, where docking was due to the electrostatic attraction, interaction

of cyt f and cyt c_6 is governed by hydrophobic forces. Moreover, whereas et reaction of cyt f

with pc follows simple collisional mechanism, cyt f and cyt c_6 displayed greater kinetic

complexity.[9,27,28,32] To further examine the et reaction between cyt f and cyt c_6 we studied

effects of temperature and viscosity on the intramolecular rate constants.

In a long-range protein et reaction it is often required that a non-et event, such as

association or rearrangement, optimize or activate the system for et. In such cases it is

difficult to ascertain whether the observed rate constant is the rate constant for the et. A

kinetic model has been developed that defines kinetically complex et reactions as true, gated

or coupled.[33-35] We analyzed the et reaction between cyt f and cyt c_6 in terms of this kinetic

model, and discovered that surprisingly all three mechanisms, true, gated, and coupled,

operate simultaneously in the cyt f and cyt c_6 system. Molecular dynamic studies, in addition

to kinetic analysis, yielded the interaction scheme in which cyt f and cyt c_6 dock into many

binding configurations where only a very few of them are et active. A diagram that plots the

distance between the electron-transfer active sites and the interaction energy of the complex

vs. the probability of occurrence shows two minima, each representing a subset of highly

populated configurations. Thus, in order to form complexes optimal for electron transfer

(judging from the distances), configurations in both subsets need to rearrange into an et

active configuration.[32] The ratio of activation free energies for this rearrangement and et

reaction determines if the reaction will proceed as true, gated or coupled. Indeed, certain

aspects of the described interaction scheme were observed previously, but never

simultaneously within one protein pair.[19,36-39]

Conclusion

The reaction between cyt f and cyt c_6 is even more interesting when contrasted with the cyt f and pc reaction. As mentioned previously, cyt c_6 and pc have similar physico-chemical properties.[6,11] Cyt c_6 and pc are both efficient in interaction with the common partners.[1,12] However, cyt c_6 exhibits far more complex kinetics in reaction with cyt f than does pc.[9,32] It is tempting to speculate that non-directional hydrophobic interaction between cyt f and cyt c_6 is the basis for the energy landscape that is suitable for such heterogeneous kinetics. More to the point, this is not the first study in which cyt c_6 and pc behave differently with a common partner, although at first glance both reactions seem equally efficient and mechanistically identical. Cyt c_6 is more efficiently cross-linked to PsaF unit of PSI (100%), than is pc. Moreover, the rate of et from cyt c_6 to PsaF in the cross-linked complex is identical to the rate of et in the native complex;[12] the strong indication that cross-linking actually captures the complex in an orientation that is already optimal for the et reaction and further rearrangement is not needed. This finding parallels the situation observed for cyt c_6/cyt f persistent complex in which one of two intracomplex reactions is viscosity independent, meaning that some of the initial docking-configurations are et active.[32] However, only about 33% of cyt c_6 cross-linked to the PsaF is able to perform et suggesting that majority of covalently captured binding configurations is not et active.[12] These configurations, although favorable for binding, obviously require rearrangement to become reactive.

A detailed understanding of how electron-transfer proteins recognize, interact, and react with each other has emerged only recently. Because the electron-transfer event occurs across a dynamic protein-protein interface, observed kinetics may depend on the geometry of

the diprotein complex, the extent of binding, and the dynamics of the docking rearrangement. This comparative study of two apparently similar proteins, cyt c_6 and pc, demonstrated that even subtle differences in binding surfaces can cause very different kinetic behavior.

References

(1) Hervas, M.; Navarro, J. A.; De la Rosa, M. A. *Accounts of Chemical Research* **2003**, *36*, 798-805.

(2) Navarro, J. A.; Hervas, M.; De la Rosa, M. A. *JBIC, Journal of Biological Inorganic Chemistry* **1997**, *2*, 11-22.

(3) Soriano, G. M.; Cramer, W. A.; Krishtalik, L. I. *Biophysical Journal* **1997**, *73*, 3265-3276.

(4) Crowley, P. B.; Ubbink, M. *Accounts of Chemical Research* **2003**, *36*, 723-730.

(5) Soriano, G. M.; Ponamarev, M. V.; Piskorowski, R. A.; Cramer, W. A. *Biochemistry* **1998**, *37*, 15120-15128.

(6) Kerfeld, C. A.; Anwar, H. P.; Interrante, R.; Merchant, S.; Yeates, T. O. *Journal of Molecular Biology* **1995**, *250*, 627-647.

(7) Gupta, R.; He, Z.; Luan, S. *Nature (London, United Kingdom)* **2002**, *417*, 567-571.

(8) Molina-Heredia, F. P.; Wastl, J.; Navarro, J. A.; Bendall, D. S.; Hervas, M.; Howe, C. J.; De La Rosa, M. A. *Nature* **2003**, *424*, 33-34.

(9) Grove, T. Ž.; Kostić, N. M. *Journal of the American Chemical Society* **2003**, *125*, 10598-10607.

(10) Gross, E. L.; Pearson, D. C., Jr. *Biophys J* **2003**, *85*, 2055-2068.

(11) Chi, Y.-I.; Huang, L.-S.; Zhang, Z.; Fernandez-Velasco, J. G.; Berry, E. A. *Biochemistry* **2000**, *39*, 7689-7701.

(12) Hippler, M.; Drepper, F.; Haehnel, W.; Rochaix, J.-D. *Proceedings of the National Academy of Sciences of the United States of America* **1998**, *95*, 7339-7344.

(13) Crowley, P. B.; Diaz-Quintana, A.; Molina-Heredia, F. P.; Nieto, P.; Sutter, M.; Haehnel, W.; De la Rosa, M. A.; Ubbink, M. *Journal of Biological Chemistry* **2002**, *277*, 48685-48689.

(14) Hippler, M.; Drepper, F.; Farah, J.; Rochaix, J.-D. *Biochemistry* **1997**, *36*, 6343-6349.

(15) Hope, A. B. *Biochimica et Biophysica Acta* **2000**, *1456*, 5-26.

(16) Anni, H.; Vanderkooi, J. M.; Mayne, L. *Biochemistry* **1995**, *34*, 5744-5753.

(17) Ye, S.; Shen, C.; Cotton, T. M.; Kostić, N. M. *Journal of Inorganic Biochemistry* **1997**, *65*, 219-226.

(18) Crnogorac, M. M.; Kostić, N. M. *Inorganic Chemistry* **2000**, *39*, 5028-5035.

(19) Pletneva, E. V.; Fulton, D. B.; Kohzuma, T.; Kostić, N. M. *Journal of the American Chemical Society* **2000**, *122*, 1034-1046.

(20) Tremain, S. M.; Kostić, N. M. *Inorganica Chimica Acta* **2000**, *300-302*, 733-740.

(21) Soriano, G. M.; Ponamarev, M. V.; Tae, G. S.; Cramer, W. A. *Biochemistry* **1996**, *35*, 14590-14598.

(22) Dikiy, A.; Carpentier, W.; Vandenberghe, I.; Borsari, M.; Safarov, N.; Dikaya, E.; Van Beeumen, J.; Ciurli, S. *Biochemistry* **2002**, *41*, 14689-14699.

(23) Ullmann, G. M.; Knapp, E.-W.; Kostić, N. M. *Journal of the American Chemical Society* **1997**, *119*, 42-52.

(24) Ullmann, G. M.; Hauswald, M.; Jensen, A.; Kostić, N. M.; Knapp, E.-W. *Biochemistry* **1997**, *36*, 16187-16196.

(25) Ubbink, M.; Ejdeback, M.; Karlsson, B. G.; Bendall, D. S. *Structure (London)* **1998**, *6*, 323-335.

(26) Ejdebaeck, M.; Bergkvist, A.; Karlsson, B. G.; Ubbink, M. *Biochemistry* **2000**, *39*, 5022-5027.

(27) Qin, L.; Kostić, N. M. *Biochemistry* **1992**, *31*, 5145-5150.

(28) Qin, L.; Kostić, N. M. *Biochemistry* **1993**, *32*, 6073-6080.

(29) Crowley, P. B.; Otting, G.; Schlarb-Ridley, B. G.; Canters, G. W.; Ubbink, M. *Journal of the American Chemical Society* **2001**, *123*, 10444-10453.

(30) Crowley, P. B.; Vintonenko, N.; Bullerjahn, G. S.; Ubbink, M. *Biochemistry* **2002**, *41*, 15698-15705.

(31) Hervas, M.; Navarro, J. A.; Diaz, A.; De la Rosa, M. A. *Biochemistry* **1996**, *35*, 2693-698.

(32) Grove, T. Ž.; Ullmann, G. M.; Kostić, N. M. **2004**.

(33) Davidson, V. L. *Accounts of Chemical Research* **2000**, *33*, 87-93.

(34) Davidson, V. L. *Biochemistry* **2000**, *39*, 4924-4928.

(35) Davidson, V. L. *Biochemistry* **1996**, *35*, 14035-14039.

(36) Lasey, R. C.; Liu, L.; Zang, L.; Ogawa, M. Y. *Biochemistry* **2003**, *42*, 3904-3910

(37) Liu, L.; Hong, J.; Ogawa, M. Y. *Journal of the American Chemical Society* **2004**, *126*, 50-51.

(38) Liang, Z.-X.; Nocek, J. M.; Huang, K.; Hayes, R. T.; Kurnikov, I. V.; Beratan, D. N.; Hoffman, B. M. *Journal of the American Chemical Society* **2002**, *124*, 6849-6859.

(39) Liang, Z.-X.; Kurnikov, I. V.; Nocek, J. M.; Mauk, A. G.; Beratan, D. N.; Hoffman, B. M. *Journal of the American Chemical Society* **2004**, *126*, 2785-2798.
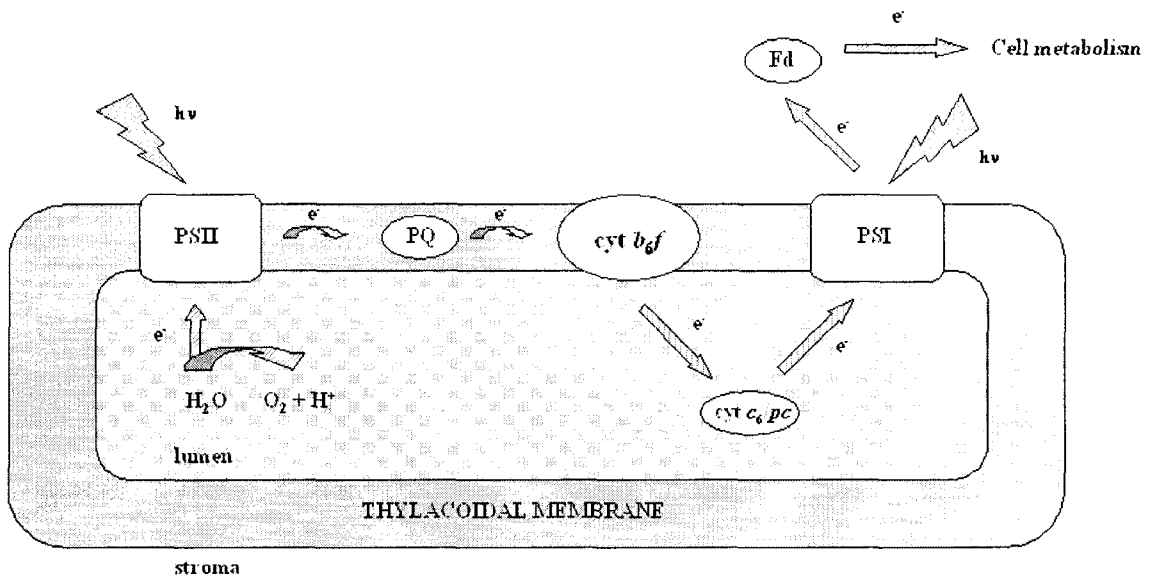
Figure 1. Linear electron flow in photosynthetic electron-transfer chain. Electrons are transferred from water to ferrodoxin by three membrane complexes PSII, cyt $b_6 f$, and PSI, which are connected by the mobile carriers plastoquinone (PQ) and cyt c_6 or pc.
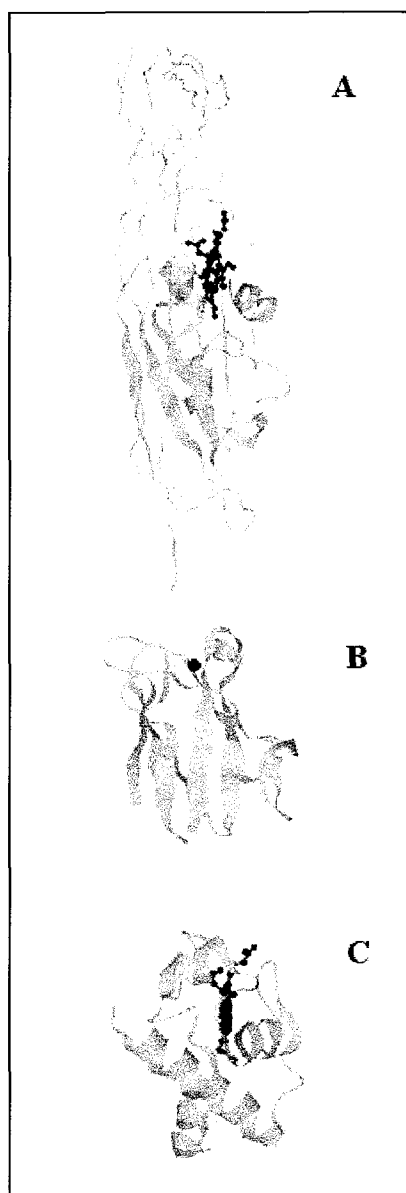
Figure 2. Tertiary structures of (A) cyt f, (B) pc, and (C) cyt c_6. Metal atoms are in the space-filling representations, porphyrin ring in ball-and-stick, and polypeptide chain in flat ribbons.

CHAPTER 5. CONCLUSIONS

Replacement of iron in cytochrome c_6 with zinc(II) ion allowed us to investigate

electron-transfer reaction between cytochrome c_6 and its physiological partner cytochrome f,

both from *Chlamydomonas reinhardtii*. We used photo-induced reaction as a tool to look at

association of these two proteins and to explore dynamics of the protein-protein interaction.

In our studies of electron transfer between ^{3}Zncyt c_6 and cyt f(III), we discovered two

distinct intracomplex processes corresponding to electron transfer within diprotein

complexes termed persistent and transient. The overall reaction remained biphasic and the

rate constants for both processes were invariant to the change of ionic strength within the

studied interval. The association constant K_a for zinc cyt c_6 and cyt f(III) remains $(5 \pm 3) \times 10^5$

M^{-1} in the ionic strength range from 700 mM to 10 mM, and than rises slightly, to $(7 \pm$

$2) \times 10^6$ M^{-1} as ionic strength is lowered to 2.5 mM. Evidently, the docking of these proteins

from *C. reinhardtii* is due to strong hydrophobic interaction slightly augmented by weak

electrostatic attraction.

As the ionic strength and the concentration of cyt f(III) in solution is raised, cyt f

increasingly associated not only with cyt c_6 but also with itself. We used covalent cross-

linking and size-exclusion chromatography to capture dimers of cyt f(III). The most

interesting feature of this apparent dimerization is the complete loss of the reactivity of

dimerized cyt f(III) toward ^{3}Zncyt c_6. We can only surmise about the significance *in vivo* of

this process. To our knowledge this is the first case in which kinetics of interprotein electron-

transfer reaction is modulated by protein self-association.

Analysis of the temperature and viscosity effects on the overall reaction between cyt

c_6 and cyt f revealed that reaction within persistent complex is true electron transfer, but

mechanism of reaction within transient complex switches from coupled to gated at the temperature of ca. 303 °K. This is the first case, to our knowledge, that same net reaction (oxido-reduction in this case) within one metalloprotein pair occurs simultaneously as true and gated, or true and coupled electron transfer. True and gated electron-transfer reactions between metalloproteins are common, but coupled reactions are still rare and are often confused with gated reactions. Here, we propose the equation that adequately treats adiabatic and nonadiabatic features of coupled mechanism. We show that the difference between three regimes, true, coupled, and gated, is not semantic but real. Furthermore, these regimes can be distinguished experimentally. The simultaneous occurrence of all three mechanisms within the same metalloprotein pair allowed us to estimate the energetics of protein interfacial rearrangement that modulates mechanism of electron-transfer reaction. Brownian dynamics calculations support dynamic picture that we infered from the kinetics studies.

Comparison of cyt c_6 and plastocyanin in their reaction with cyt f revealed that the identical function and seemingly very similar physico-chemical properties of the two proteins are not a guarantee that the common reaction will follow a common mechanism. Brownian dynamics simulation offers broad picture of possible binding configurations between two proteins. However, in kinetics experiments only configurations that are reactive are observable. The stark difference between cyt c_6/ cyt f and plastocyanin/cyt f pair is that in the former mainly hydrophobic forces govern docking into reactive configurations, while in the later electrostatic attraction is responsible for protein association.

Specific recognition and binding between proteins occur widely in biological systems. The studies included in this dissertation show how kinetics can be used as a tool to develop a physical picture of the interaction between two electron-transfer proteins. Many

aspects of the discussion presented here are applicable to protein-protein interactions in general.

APPENDIX

Preparation of Zinc Cytochrome c_6

Electron-transfer reactions of metalloproteins play an essential role in many biological processes. Detailed study of their molecular mechanism is interesting from a biological, chemical, and biophysical points of view. The diverse factors that govern reactions in vivo, at the cellular level, can be separated and studied in vitro, at the molecular level [1-4].

Various heme proteins are ubiquitous in biological systems. The problem of studying thermal redox reaction between two heme proteins lays in the fact that their absorption spectra overlap [5,6]. This makes spectrophotometrical monitoring of changes in oxidation states difficult. A solution to this problem is to replace redox-active iron in the heme by redox-inactive zinc(II), so that the redox step becomes photoinduced.

Just as the peptide part of the protein can be modified by means of mutagenesis, so the active site of the protein can be modified by methods of coordination chemistry. Derivatives of cytochromes containing various metals in the place of iron have been characterized and used to probe structure, function, and reactivity of these proteins. Zinc cytochrome c has been used in kinetic studies of electron-transfer reactions in our and other laboratories [1,2,7-14].

Especially useful for kinetic studies is the lowest-lying triplet excited state. Its lifetime is between 7 and 15 ms, depending on the protein purity. Because the lifetime is relatively long, redox quenching of this excited state can be studied easily. The advantages of zinc substituted cytochromes are multiple. Because excited triplet-state can be easily created

by the laser, no external reducing agents are needed. Thus the interpretation of results is straightforward. Moreover, the triplet state of zinc cytochromes is much stronger reductant than the native protein [5,8].

Here we present the procedure for zinc reconstitution of cytochrome c6. Cytochrome c6 is a c-type cytochrome. The heme is covalently attached to the protein backbone through two cysteines. Axial ligands to iron are nitrogen form the histidine and sulfur from the metionine [15]. The cytochrome c6 closely resembles cyt c in its heme binding and iron coordination, so the procedure presented is a modification of the original procedure for reconstitution of cytochrome c [16,17].

Experimental Procedure.

All experiments involving hydrogen fluoride were done inside the hood. The researcher was protected with a respiration mask, eye goggles, a face shield, two pairs of gloves (latex and rubber), laboratory coat, and plastic apron. All experiments involving metal-free cytochrome c6, and zinc cytochrome c6 were done in dark or under the red light.

The protein solution was dialyzed against the water to remove buffer and salts and then lyophilyzed. About 5mg of the protein powder was placed into the Teflon beaker through a cone of glassy paper. The beaker was submerged into a Dewar holding liquid nitrogen. Subsequent steps were done under the red light. Hydrogen fluoride gas from the lecture bottle was passed through the Teflon tubing into the open beaker for about 40 seconds. The beaker was removed from the liquid nitrogen and the content was stirred with a Teflon rod until melted. The beaker was again placed in the liquid nitrogen and hydrogen fluoride gas was passed into it for additional 30 seconds. The Teflon beaker was removed from the liquid nitrogen and the content was stirred with the Teflon rod until melted and then for additional 3 to 5 minutes. The small amount of residual HF in the Teflon beaker was

removed by a current of ultrapure argon. The argon was stopped when white fumes no longer

emerged from the beaker. The exposure of the solution to the current of argon will reduce the

solution volume, care should be taken not to dry it out. The solution was resuspended in the

total volume of 2 ml of 20 mM acetate buffer + 8M urea, pH 5.2. Solution was loaded onto

the Bio-Rad prepacked PD 10 desalting column, equilibrated with the 20 mM acetate buffer

+ 8M urea, pH 5.2 (equilibrate column immediately before use). The protein was eluted with

the same buffer and entire colored fraction was collected. The visible absorption spectrum of

the effluent was recorded. Metal-free cytochrome c6 (H2cytc6) has characteristic peaks at

506, 540, 568, and 620 nm (Figure 1).

Approximately tenfold excess of zinc acetate was added to the solution of metal-

free cytochrome c6 and mixture was kept in a water bath at 40°C for ca. 30 minutes.

Completion was checked by visible absorption spectra. As H2cytc6 was converted to

Zncytc6, the bands of the former disappeared and those of latter, at 423, 549, and 585 nm,

appeared, as illustrated in Figure 1. The resulting clear solution was then dyalized against

water, to remove urea and excess zinc acetate, and then against desired buffer. The protein

was purified on DEAE-cellulose column with a 20 mM sodium acetate buffer + 100 mM

sodium chloride, pH 5.2 as the eluent. Usually only one band was evident.

Absorptivities of zinc cytochrome c_6, $\Delta\varepsilon_{421}=(2.3\pm0.1)\times10^5$ $M^{-1}cm^{-1}$, was determined

from absorption spectra and quantification of total protein using the BCA protein assay

reagent kit. The triplet state was excited with the second harmonic (at 532 nm) of a Q-

switched Nd-YAG laser. Argon was passed first through water and then through the buffer

solution. The required volume of buffer was deaerated in a 10-mm cuvette for at least 30

minutes before zinc cytochrome c_6 was added. Decay of the triplet state was monitored at

460 nm, where the transient absorbance reaches the maximum. In the absence of a quencher,

the natural decay of the triplet excited state of the porphyrin to its ground state, lifetime, is

monoexponential. The rate constant, k_{nd}, is 100 ± 10 s^{-1} at room temperature in phosphate

buffer having pH 7.00 and is independent of protein concentration in the interval from 1.0 to

10 μM and of ionic strength in the interval from 2.5 to 700 mM.

The Zncyt c6 was characterized with circular dichroism (CD) spectroscopy. CD in

the far-UV range is the property of the protein backbone and is sensitive indicator of the

protein conformation [17]. We compared the spectra of cytochrome c6 containing iron(III),

iron(II), and zinc(II) ions in the porphyrin. As the superimposed spectra in Figure 2 show, the

three forms of cytochrome c6 have nearly identical conformations. This result shows that

replacement of iron by zinc(II) does not cause any significant conformational change in
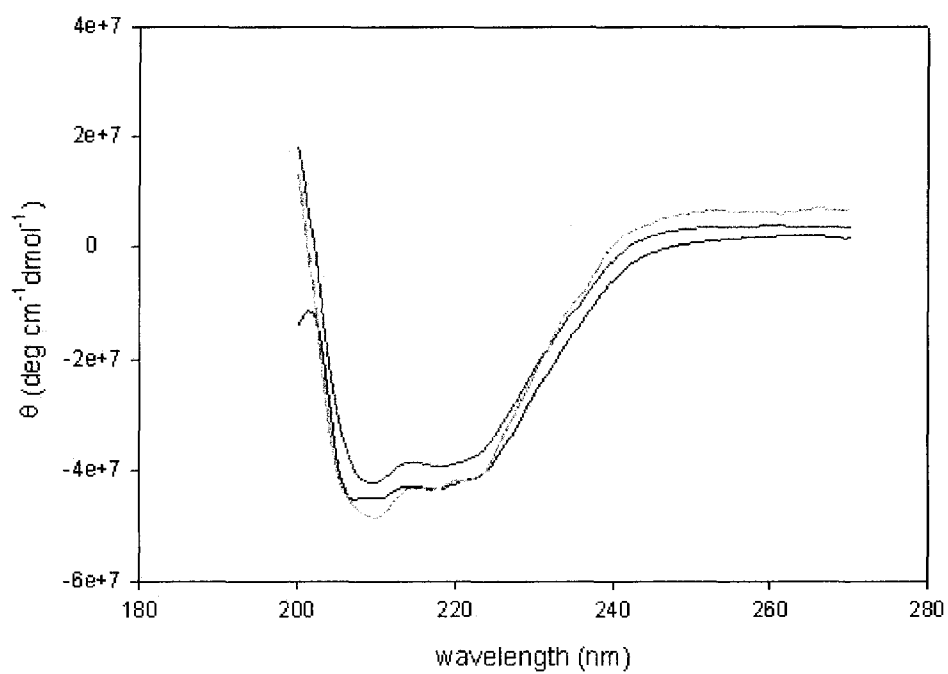
cytochrome c6.

References

(1) Liang, Z.-X.; Nocek, J. M.; Huang, K.; Hayes, R. T.; Kurnikov, I. V.; Beratan, D. N.;

  Hoffman, B. M. *Journal of the American Chemical Society* **2002**, *124*, 6849-6859.

(2) Pletneva, E. V.; Fulton, D. B.; Kohzuma, T.; Kostić, N. M. *Journal of the American

  Chemical Society* **2000**, *122*, 1034-1046.

(3) Crowley, P. B.; Ubbink, M. *Accounts of Chemical Research* **2003**, *36*, 723-730.

(4) Davidson, V. L. *Accounts of Chemical Research* **2000**, *33*, 87-93.

(5) Tremain, S. M.; Kostić, N. M. *Inorganica Chimica Acta* **2000**, *300-302*, 733-740.

(6) Hervas, M.; Navarro, J. A.; De la Rosa, M. A. *Accounts of Chemical Research* **2003**, *36*,

  798-805.

(7) Crnogorac, M. M.; Shen, C.; Young, S.; Hansson, O.; Kostić, N. M. *Biochemistry* **1996**, *35*, 16465-16474.

(8) Crnogorac, M. M.; Kostić, N. M. *Inorganic Chemistry* **2000**, *39*, 5028-5035.

(9) Ivković-Jensen, M. M.; Ullmann, G. M.; Crnogorac, M. M.; Ejdebaeck, M.; Young, S.; Hansson, O.; Kostić, N. M. *Biochemistry* **1999**, *38*, 1589-1597.

(10) Pletneva, E. V.; Crnogorac, M. M.; Kostić, N. M. *Journal of the American Chemical Society* **2002**, *124*, 14342-14354.

(11) Zhou, J. S.; Tran, S. T.; McLendon, G.; Hoffman, B. M. *Journal of the American Chemical Society* **1997**, *119*, 269-277.

(12) Liang, Z.-X.; Kurnikov, I. V.; Nocek, J. M.; Mauk, A. G.; Beratan, D. N.; Hoffman, B. M. *Journal of the American Chemical Society* **2004**, *126*, 2785-2798.

(13) Grove, T. Ž.; Kostić, N. M. *Journal of the American Chemical Society* **2003**, *125*, 10598-10607.

(14) Ivković-Jensen, M. M.; Kostić, N. M. *Biochemistry* **1997**, *36*, 8135-8144.

(15) Kerfeld, C. A.; Anwar, H. P.; Interrante, R.; Merchant, S.; Yeates, T. O. *Journal of Molecular Biology* **1995**, *250*, 627-647.

(16) Anni, H.; Vanderkooi, J. M.; Mayne, L. *Biochemistry* **1995**, *34*, 5744-5753.

(17) Ye, S.; Shen, C.; Cotton, T. M.; Kostić, N. M. *Journal of Inorganic Biochemistry* **1997**, *65*, 219-226.
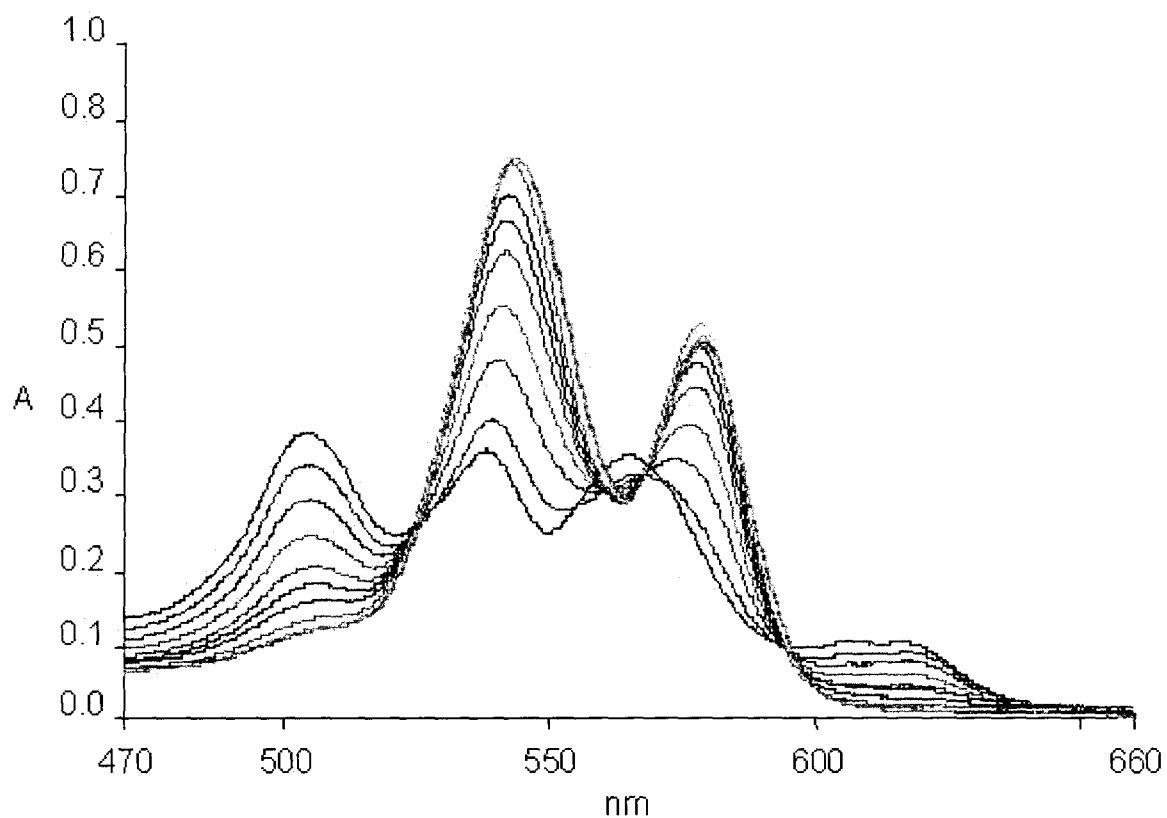
Figure 1. Time course of the reconstitution of the "free-base" cyt c_6 with zinc (II) ions. Absorption spectrum of H_2cyt c_6 is shown as a blue line (t = 0) and absorption spectrum of Zncyt c_6 is shown as a green line (t = 30 min).

Figure 2. Circular dichroism spectra of the the ferricytochrome c_6 (pink), ferrocytochrome c_6 (black), and zinc cytochrome c_6 (green).

ACKNOWLEDGEMENTS